Research Square

Preprints are preliminary reports that have not undergone peer review.
They should not be considered conclusive, used to inform clinical practice,
or referenced by the media as validated information.

Local land use and landscape heterogeneity reduce tropical biodiversity and multifunctionality

Zheng Zhou

zheng.zhou@uni-hohenheim.de

University of Hohenheim

Catrin Westphal

University of Göttingen https://orcid.org/0000-0002-2615-1339

Jochen Drescher

University of Goettingen https://orcid.org/0000-0002-5162-9779

Valentyna Krashevska

Senckenberg

Arne Wenzel

Functional Agrobiodiversity & Agroecology, University of Göttingen

Kevin Darras

INRAE https://orcid.org/0000-0002-9013-3784

Christian Stiegler

Earth Sciences New Zealand

Michael Schlund

University of Twente https://orcid.org/0000-0001-6657-6713

Fabian Brambach

University of Göttingen https://orcid.org/0000-0002-3203-2248

Anton Potapov

Senckenberg

Carina Moura

Forest Genetics, The University of Freiburg

Martyna Kotowska

Macquarie University https://orcid.org/0000-0002-2283-5979

Kibrom Sibhatu

International Center of Insect Physiology and Ecology (icipe)

Ashehad Ali

New Zealand Institute for Bioeconomy Science Limited

Desi Anggrahini

Department of Plant Protection, Faculty of Agriculture, IPB University

Clemens Anschütz

Ecology of Tropical Agricultural Systems, University of Hohenheim

damayanti buchori

Bogor Agricultural University https://orcid.org/0000-0002-2843-0737

Ting-Wen Chen

Animal Ecology, JF Blumenbach Institute of Zoology and Anthropology, University of Göttingen https://orcid.org/0000-0001-9449-3034

Naufal Dhiya'ulhaq

Universitas Gadjah Mada

Patrick Diaz

University of Jambi, Jambi, indonesia

Purnama Hidayat

IPB University https://orcid.org/0000-0001-9507-6275

Thomas Hiller

Ecology of Tropical Agricultural Systems, University of Hohenheim

Indah Indah

Department of Plant Protection, Faculty of Agriculture, IPB University

Svea Jahnk

"Department of Palynology and Climate Dynamics, Albrecht-von-Haller Institute for Plant Sciences University of Göttingen"

Kasmiatun Kasmiatun

IPB University

Zuopeng Liu

Animal Ecology, JF Blumenbach Institute of Zoology and Anthropology, University of Göttingen, Göttingen, Germany;

Aulia Maulidya

Department of Plant Protection, Faculty of Agriculture, IPB University

Siti Meliah

Department of Genomic and Applied Microbiology, Institute of Microbiology and Genetics, Georg-August-University, Göttingen, Germany https://orcid.org/0000-0002-7030-6369

Yeni Mulyani

Bogor Agricultural University IPB

Rizky Nazarreta

https://orcid.org/0000-0003-4222-411X

Chung Nguyen

Department of Palynology and Climate Dynamics, Albrecht-von-Haller Institute for Plant Sciences, University of Göttingen

Pallavi Pallavi

Tropical Silviculture and Forest Ecology, University of Göttingen

Gustavo Paterno

University of Göttingen https://orcid.org/0000-0001-9719-3037

Nathaly Guerrero-Ramírez

Biodiversity, Macroecology and Biogeography, Faculty of Forest Sciences and Forest Ecology, University of Göttingen https://orcid.org/0000-0001-7311-9852

M. Naufal Rizqulloh

Animal Ecology, JF Blumenbach Institute of Zoology and Anthropology, University of Göttingen

Jacob Schmidt

Forest Botany and Tree Physiology, University of Göttingen

Iskandar Siregar

Department of Silviculture, Faculty of Forestry and Environment, IPB University

Winda Susanti

Johann Friedrich Blumenbach Institute of Zoology and Anthropology, University of Göttingen, Goettingen, Germany

Sri Tjitrosoedirdjo

SEAMEO-BIOTROP

Aiyen Tjoa

Fakultas Pertanian, Universitas Tadulako

Triadiati Triadiati

Department of Biology, Faculty of Mathematics and Natural Sciences, IPB University

Gennuo Wang

Animal Ecology, JF Blumenbach Institute of Zoology and Anthropology, University of Göttingen

Simin Wang

Animal Ecology, JF Blumenbach Institute of Zoology and Anthropology, University of Göttingen

Xu Xu

Animal Ecology, JF Blumenbach Institute of Zoology and Anthropology, University of Göttingen

Haifeng Yao

State Key Laboratory of Regional and Urban Ecology, Ningbo Observation and Research Station, Institute of Urban Environment, Chinese Academy of Sciences

Ellena Yusti

EFForTS, University of Jambi

Behling Hermann

University of Göttingen

Rolf Daniel

Georg-August-university of Göttingen https://orcid.org/0000-0002-8646-7925

Stefan Erasmi

Thünen Institute of Farm Economics

Oliver Gailing

University of Göttingen https://orcid.org/0000-0002-4572-2408

Dirk Hölscher

University of Göttingen https://orcid.org/0000-0002-7097-3102

Alexander Knohl

University of Goettingen https://orcid.org/0000-0002-7615-8870

Andrea Polle

Georg-August Universität Göttingen https://orcid.org/0000-0001-8697-6394

Matin Qaim

University of Bonn https://orcid.org/0000-0003-4143-0763

Teja Tscharntke

University of Göttingen

Kerstin Wiegand

University of Göttingen

Holger Kreft

University of Göttingen https://orcid.org/0000-0003-4471-8236

Stefan Scheu

JF Blumenbach Institute of Zoology and Anthropology, University of Göttingen https://orcid.org/0000-0003-4350-9520

Ingo Grass

University of Hohenheim https://orcid.org/0000-0001-7788-1940

Biological Sciences - Article

Keywords:

Posted Date: June 3rd, 2026

DOI: https://doi.org/10.21203/rs.3.rs-9563760/v1

License: This work is licensed under a Creative Commons Attribution 4.0 International License.
Read Full License

Additional Declarations: There is **NO** Competing Interest.

Abstract

Tropical rainforests harbor exceptional biodiversity and function, but are increasingly threatened by agricultural expansion. Whether landscape heterogeneity mitigates these impacts, as in temperate systems, remains unclear. Here, we quantified how local land use and landscape heterogeneity shape multidiversity and ecosystem multifunctionality, using 34 biodiversity metrics and 21 functions across 128 plots in Sumatra. Relative to rainforests, plantations reduced multidiversity and multifunctionality by ~25%, with stronger aboveground declines, lower plant and animal but higher microbial diversity. Contrary to temperate systems, landscape heterogeneity did not buffer local land-use effects but exacerbated declines in multidiversity and multifunctionality, and benefits of surrounding-rainforest cover were confined to rainforest fragments rather than plantations. Our results highlight the irreplaceability of continuous tropical rainforests, and the limited transferability of temperate-based landscape conservation strategies.

Main

Tropical rainforests, while covering <7% of Earth's land surface, harbor a disproportionate share of global terrestrial biodiversity and underpin key ecosystem functions including carbon sequestration and climate regulation[1–3]. Despite their global significance, tropical rainforests are disappearing at an alarming rate[4,5]. Agricultural expansion is one of the major drivers of tropical deforestation[6,7], converting hyperdiverse rainforests into simplified agricultural systems dominated by cash crops[8]. While these tropical land-use systems provide income, employment and commodities to local communities and global markets, their expansion entails pronounced social-ecological trade-offs, eroding local biodiversity and compromising ecosystem functioning[9].

Traditional strategies to conserve tropical biodiversity and ecosystem functioning have centered on retaining or restoring natural forests[10,11]. However, given rapid habitat loss and acute socio-economic needs, relying solely on large-scale forest protection is increasingly unfeasible. A complementary paradigm, largely derived from agricultural landscapes of the temperate regions, particularly Europe, emphasizes the critical role of landscape heterogeneity[12,13]. Beyond the well-established benefits of increasing natural habitat cover at the landscape level, numerous studies from temperate regions suggest that the landscape compositional and configurational heterogeneity of different land-use types is also vital for sustaining biodiversity and ecosystem services, prompting the adoption of these concepts in major global sustainability frameworks (e.g., FAO, IPBES)[14,15]. However, whether these temperate-derived strategies also apply to the tropics, characterized by distinct biota and land-use histories, represents a critical gap with direct implications for conserving the world's most biodiverse regions.

Furthermore, most studies on land-use effects on tropical biodiversity or ecosystem functions have focused on individual taxa or single functions[16], thereby failing to capture the complex, multidimensional

nature of whole-ecosystem responses[17,18]. Specifically, aboveground taxa and their associated functions tend to experience stronger negative effects of land-use intensification than belowground communities[19]. Likewise, plant and animal diversity often decline with agricultural expansion[20,21], whereas microbial diversity may even increase under certain conditions[22,23]. Therefore, to achieve effective conservation and sustainable land-use planning in the hyperdiverse tropical regions, it is necessary to consider multiple taxa and ecosystem functions, as reflected by multidiversity and multifunctionality[17,18], to capture the full range of impacts of land-use change and associated landscape modifications.

Can temperate-derived landscape strategies be translated to the tropics? We addressed this question in heterogeneous tropical lowland landscapes of Jambi Province in Sumatra, Indonesia (Figs 1a, S1, Table S1). Rainforests in Sumatra have been extensively converted into managed plantations over recent decades[24]. Industrial estates and smallholder farms now co-occur across the region, creating a gradient from homogeneous to highly heterogeneous landscapes, and making it a powerful model case of tropical land-use change. Based on evidence from temperate landscapes, we hypothesized that

(i) conversion from rainforest to plantations reduces both multidiversity and ecosystem multifunctionality, with stronger aboveground declines due to vegetation simplification and microclimatic shifts[19];

(ii) higher compositional and configurational heterogeneity enhances multidiversity and multifunctionality via habitat complementarity, spillover, and rescue effects[12,13], especially in intensive plantations; and

(iii) greater rainforest cover at the landscape scale increases local biodiversity and ecosystem functioning, especially in plantations, by supplying source populations and promoting recolonization.

To test these hypotheses, we utilized a comprehensive dataset from 128 study plots spanning a landscape gradient of four major land-use types: rainforest, shrubland, rubber and oil palm monoculture plantations. We compiled 34 biodiversity indicators (52,751 species across 16 taxonomic groups spanning microorganisms, plants, and animals) and 21 ecosystem functions (e.g., energy flux, litter decomposition). Based on these measurements, we derived metrics of multidiversity and ecosystem multifunctionality of the whole ecosystem, as well as different compartments (i.e., above- and belowground, different kingdoms and functional classifications), which capture ecosystem complexity more holistically than single metrics and thus better inform management and conservation[17,18]. Furthermore, we quantified landscape compositional and configurational heterogeneity, namely landscape diversity and edge density, within circular buffers from 100 m up to 3000 m surrounding each study plot. By compiling these datasets, we investigated the local land-use and landscape-heterogeneity effects on tropical biodiversity and ecosystem functions across the tropical lowland landscapes.

Multidiversity and multifunctionality decline after land use at local scale

Confirming our first hypothesis, local multidiversity and multifunctionality were consistently lower in all other land-use types than in rainforests, regardless of the calculation method (average or threshold-based, Figs 2, S1, S2). Compared to rainforest, rubber and oil palm plantations showed pronounced reductions in multidiversity (−21.5% and −24.8%) and multifunctionality (−22.6% and −23.8%), while shrubland exhibited modest declines in multidiversity (−6.1%) and multifunctionality (−10.3%), emerging as an intermediate habitat.

The effects of land use (plantations vs. rainforest) were generally negative for aboveground taxa and ecosystem functions and became neutral or positive belowground (Figs 1b, S2), ranging from substantial losses in trees (−89% species/plot) to substantial gains in rhizosphere fungi (+72% species/plot) (Fig. 1b). Ecosystem functions showed a comparable pattern, shifting from sharp decreases in air-humidity stability (−74%) to increases in saturated photosynthesis (+44%) (Fig. 1b). Overall, land-use effects on multidiversity and multifunctionality were stronger for aboveground than belowground taxa and functions (Figs 2, S4, S5), consistent with findings from temperate regions[19]. Multidiversity response was structured across microhabitats along the vertical dimension, ranging from −46% in the canopy and −23% in the litter to non-significant changes in the rhizosphere, and positive ones in the soil (+10%) (Fig. S6). This pattern likely arises because aboveground organisms are directly exposed to changes in habitat structure and land-use disturbances (e.g., vegetation removal or microclimate shifts), while belowground biota may be less directly exposed to such disturbances[19,25]. Besides, the land-use effects generally increased as stricter thresholds were applied in the multidiversity and multifunctionality calculation (Figs S4, S5), supporting the use of higher thresholds to align evaluations with more stringent conservation objectives[20,26].

The local land-use conversion gradient mainly decreased plant and animal diversity but had neutral or positive effects on microorganisms (Figs 1b, S2), thereby decreasing plant and animal multidiversity while increasing microbial multidiversity (Figs 3, S4). These differences likely arise from distinct pathways of land-use impacts on resources and habitat structure. Plant diversity declined in plantations through replanting and herbicide application[27], reducing host richness and simplifying vegetation and microhabitat structure. These bottom-up losses in plant resources contract trophic and habitat niches available to animals[27,28]. By contrast, land use often elevates soil pH, mitigating aluminum toxicity under acidic conditions[29,30] and thereby reducing physiological stress on microbial communities[31]. Meanwhile, fertilization and repeated mechanical weed control can increase the quantity and quality of resources entering the soil, by raising the availability of inorganic nitrogen and labile carbon and by generating repeated inputs of high-quality plant residues, thereby favoring copiotrophic taxa and enhancing microbial activity and diversity[32,33]. Overall, the land-use changes generate opposing diversity responses through distinct mechanisms across above- and belowground communities and among taxonomic groups.

Furthermore, local land use weakened key ecosystem functions related to ecosystem productivity, energy flux and microclimatic stability (Figs 3, S5). Decreases in tree biomass and simplification of vegetation structure led to lower primary production[34], which in turn lowers energy transfer to higher trophic levels and weakens the capacity of ecosystems to buffer environmental disturbances[35]. These changes signal an erosion of the system's ability to sustain biodiversity and ecosystem services over time. Nutrient cycling was not significantly affected by land use (Figs 3, S5), likely because it is driven largely by soil microbial processes that are stimulated under plantation management through higher pH and fertilization[31]. In addition, the relatively labile herb and weed litter in plantations may decompose rapidly, thereby contributing to the maintenance of nutrient cycling[36].

Multidiversity and multifunctionality decrease in more heterogeneous landscapes

Contrary to our second hypothesis, higher landscape heterogeneity, both compositional heterogeneity (i.e., Shannon diversity of land-use types) and configurational heterogeneity (i.e., edge density), was negatively associated with the plot-level aboveground multidiversity, especially at broader spatial scales (Figs. 4, S7–S8). As interactions between landscape heterogeneity metrics were rare in the exploratory full models, we focused on main effects here (detailed in Methods). This finding contrasts with a large number of studies from temperate regions, where higher landscape heterogeneity is typically considered to benefit local biodiversity, e.g., via increasing the landscape species pool and resource complementation in more diverse landscapes[12,37] or by facilitating dispersal and spillover among adjacent habitats through greater edge density[38,39].

These contrasting patterns may be shaped by differences not only in land-use history, but also in the evolutionary and biogeographic context of temperate and tropical regions. Most large-scale studies on the effects of landscape heterogeneity on biodiversity have focused on temperate agroecosystems in Europe and North America[13,40], where centuries of land use have led to the widespread disappearance of species incompatible with human land use, while disturbance-tolerant and synanthropic species have benefited[41,42]. In addition, repeated Pleistocene climatic fluctuations and shifts between forested and open biomes[43,44] may have favored temperate biota that are more tolerant of environmental variability and habitat turnover[45]. Moreover, many temperate agricultural landscapes retain elements that are structurally or functionally closer to naturally open or semi-open ecosystems, such as grasslands and light woodlands[46,47]. However, in most tropical regions, including our study region in the Sumatran lowlands, the large-scale conversion of tropical rainforests into monoculture plantations has occurred mainly in recent decades[8,11]. Consequently, as explained by extinction-filter theory[42], species assemblages in such recently transformed tropical landscapes may retain a larger proportion of forest-dependent and disturbance-sensitive taxa, lacking traits that confer tolerance to anthropogenic activities and therefore being particularly vulnerable to the rapid expansion of agriculture. Furthermore, higher heterogeneity in temperate zones often means increased proportions of (semi-)natural habitats in

agricultural landscapes, forming a mosaic of complementary habitats[48,49]. By contrast, high compositional heterogeneity in the Sumatran lowlands rather reflects the proliferation of non-forest land-use types within a largely inhospitable agricultural matrix. These land-use, evolutionary and biogeographic differences fundamentally reframe how landscape heterogeneity should be interpreted in the tropics.

In contrast to aboveground biodiversity, belowground multidiversity exhibited no significant response to landscape heterogeneity (Fig. 4), which is likely due to its assembly being governed by fine-scale edaphic filters that function relatively independently of patch configuration. Soil physiochemistry, especially pH, has been identified as the strongest predictor of global soil-microbial diversity, often explaining 20–40% of community variation[50,51]. Furthermore, active dispersal in many soil taxa is also limited to centimeters or in larger species to meters[52], implying that the spatial grain at which heterogeneity impacts them is far smaller than the landscape buffers used here. Aboveground taxa, by contrast, experience the landscape at larger spatial scales, where dispersal, mass effects and source–sink dynamics can couple local communities to landscape composition and configuration[38,53]. Consequently, landscape heterogeneity can be expected to be more influential in structuring aboveground than belowground biodiversity.

Landscape heterogeneity metrics were also negatively associated with plot-level multifunctionality (Fig. 4b, Figs S9–S10). This decline in ecosystem functioning is likely mediated by biodiversity loss[54,55], as reduced species richness and altered community composition can weaken the complementarity and redundancy among taxa that sustain key ecological processes[56]. Such biodiversity-functioning linkages can extend beyond local communities to the metacommunity level across spatially structured landscapes[57]. The high land-use intensity in the study landscapes likely eroded the metacommunity dynamics needed to sustain biodiversity, whereas such dynamics may be better maintained in temperate landscapes with more extensive land use and synanthropic species, allowing species and associated ecosystem functions to sustain across heterogeneous landscapes.

Landscape-scale rainforest cover promotes local multidiversity and multifunctionality in rainforest fragments but not oil palm plantations

Initial statistical models revealed a significant interaction between rainforest cover and land-use type for both multidiversity and multifunctionality (Figure S11), leading us to conduct subsequent analyses separately for each land-use type. Contrary to our third hypothesis, the amount of remaining rainforest cover at the landscape scale was positively associated with local aboveground multidiversity in rainforest fragments and shrublands but not in plantations (Fig. 5, S11). Again, these findings contrast with extensive evidence from temperate regions, where surrounding natural habitats generally enhance local biodiversity within agroecosystems, primarily via species spillover, source-sink dynamics and the

provision of additional resources[37,40,58]. Compared with temperate regions, tropical forest biota has experienced relatively low historical exposure to anthropogenic disturbances[59]; these historical differences may have contributed to narrower niche breadths, smaller ranges, and lower effective dispersal for many tropical forest taxa, which may in turn reduce spillover into plantations[42]. Furthermore, the low species overlap between forests and plantations (< 20% in canopy ant, beetle, spider, wasp and bird species in the same region[60–64] and other tropical study[65]) indicates strong filtering of tropical specialist taxa, limits the contribution of surrounding rainforest to species communities within plantations. This pattern is consistent with a recent study reporting that neighboring forest fragments contribute only marginal biodiversity spillover to oil palm plantations in the Brazilian Amazon[66]. Our results suggest that surrounding rainforest could not overcome the strong environmental filtering imposed by intensive plantations, highlighting a key contrast with temperate landscapes where adjacent seminatural habitats often enhance farmland diversity.

Meanwhile, rainforest fragments and shrublands surrounded by additional rainforest patches were characterized by higher multidiversity (Fig. 5, Fig. S11). This pattern suggests that these habitats remain connected to the regional forest species pool, consistent with the “source–sink” perspective of metacommunity theory[38,67]. Increased forest cover is expected to enhance colonization by forest specialists, generating rescue effects that lower local extinction risk[68,69]. In contrast, plantations contributed little to biodiversity in neighboring forests, indicating that the heterogeneity generated by transforming extensive forest areas into plantations fails to contribute to forest biodiversity or ecosystem functioning. Intensively managed plantations, characterized by high chemical inputs and reduced structural complexity, may even act as sinks for forest biodiversity within the tropical landscape matrix[70,71]. These findings underscore the irreplaceability of primary rainforest and highlight that even small rainforest fragments embedded in agricultural matrices can be disproportionately valuable by supporting metapopulation connectivity and persistence among remnant forest patches.

Conclusions

Our study challenges the universal applicability of temperate-derived conservation strategies by demonstrating that local land use and landscape heterogeneity fundamentally drive biodiversity loss and ecosystem degradation in the tropics, with stronger effects aboveground than belowground. In contrast to patterns commonly reported from temperate regions, we found that greater landscape compositional and configurational heterogeneity was associated with declines in local multidiversity and multifunctionality. Furthermore, greater landscape-level rainforest cover supported local multidiversity and multifunctionality in rainforest fragments, but not in oil palm plantations, underscoring both the irreplaceability of tropical primary forests and the substantial challenges for tropical biodiversity conservation once rainforest has been converted into plantations. Overall, our results suggest that adopting agroecological strategies and conservation frameworks from the temperate regions is inadequate to foster multidiversity and multifunctionality in the tropics. Rather, they highlight the

overwhelming importance in targeting efforts towards the conservation of rainforest and rainforest fragments for the conservation of biodiversity and ecosystem functions in the tropics.

Methods

The landscape assessment experiment

We conducted a large-scale, interdisciplinary landscape assessment ("EFForTS-LA") in Sumatra, Indonesia, which is part of the EFForTS project: Ecological and Socioeconomic Functions of Tropical Lowland Rainforest Transformation Systems[24]. We established a total of 128 study plots across a ~6800 km² region in Jambi province, Sumatra, which encompasses the last major remnants of lowland rainforest in the area (Bukit Duabelas National Park and Harapan Rainforest/ PT Restorasi Ekosistem Indonesia REKI). The plots were distributed across four major land-use types: rainforest, shrubland, rubber and oil palm plantations (32 plots per land-use type). Plot selection followed a stratified design to capture key ecological and socio-economic gradients, including plantation age, surrounding forest cover, land ownership and migration background, and management intensity (Table S1, Figure S1). Plots were distributed across multiple regions (Batanghari, Bukit Duabelas, Pematang Kabau, and Harapan/REKI) to disentangle land use from regional effects.

Land-use types were defined by vegetation structure and canopy closure: forests with >50% canopy closure; shrubland as fallows or regenerating areas with up to 50% canopy closure; rubber systems ranging from monocultures to jungle rubber agroforests; and oil palm plantations managed either by smallholders or company estates. The plot network was designed to cover independent gradients of local land-use intensity and surrounding landscape heterogeneity (250–3000 m radii), thereby enabling analyses of both local- and landscape-scale drivers of biodiversity and ecosystem functioning. Each plot was circular with a radius of 18 m (≈1000 m^2) and contained five geo-referenced subplots (one central and four peripheral subplots in the cardinal directions), each with a radius of 2.82 m (25 m^2). Subplots were permanently marked to allow re-sampling, with a minimum spacing of 12.2 m to ensure comparability and minimize edge effects. This standardized layout provides a consistent framework for assessing biodiversity and ecosystem functions across contrasting land-use types and management systems.

Field measurements

The campaign was designed to ensure standardized data collection across all 128 plots while covering a broad range of biotic and abiotic components, including vegetation structure, soil properties and microorganisms, fauna, pollinators, microclimate, and ecosystem processes. Given the size and multidisciplinary scope of the project, the sampling campaign was organized as a coordinated effort involving multiple research groups and methodological approaches. To ensure comparability among subprojects, all sampling was conducted within the same set of plots and followed harmonized spatial

scales and timelines. Field teams were organized into functional groups (e.g., vegetation, soil, fauna, microclimate), with staggered schedules to minimize interference between sampling activities. Each group followed standardized protocols but coordinated their work through a joint schedule to achieve efficient data collection while maintaining methodological consistency.

Biodiversity metrics

Birds

Bird vocalizations were recorded using automated sound recorders (SM2Bat+, Wildlife Acoustics Inc., USA equipped with Pavo microphones). Recorders were mounted on poles at the centre of each sampling plot and deployed once per location between May and December 2021. At each site, recordings started 1 h before local sunrise and continued for 4 h, covering the peak period of avian vocal activity. Audio was sampled at 44.1 kHz on both channels (stereo recordings). Bird species were identified using BirdNET Analyzer (version 2.4;[72]). Analyses were run using the standard BirdNET settings for detection sensitivity (1) and confidence threshold (0.1), with a 2-s overlap between consecutive analysis windows. Species predictions were restricted to a manually curated list of locally occurring bird species to reduce false positives. All automated species identifications were subsequently validated following the procedure described by Wood & Kahl[73]. Validation involved manual inspection of sonograms and acoustic verification of 50 randomly selected detections per species spanning a range of confidence scores, ensuring high reliability of species occurrence data derived from automated classifications.

Bats

Insectivorous bat calls were recorded using automated sound recorders (SM2Bat+, WIldlife Acoustics Inc., USA, equipped with Pavo microphones). Recorders were mounted on poles at the centre of each sampling plot and deployed once per location between May and December 2021. At each site, recordings started at sunset and continued for four hours, covering the first peak of bat echolocation activity. Audio was sampled at 384 kHz (high-pass filter: 3 Hz) on one channel (mono recordings). From these recordings, two rain-free 10-min segments per site were selected, beginning 30 minutes after sunset. Selected files were uploaded to the ecoSound-web platform, where clearly identifiable bat calls were manually tagged by a trained observer and subsequently reviewed by experienced bat taxonomists to ensure data quality. Only validated calls were retained for analysis. To standardize detection areas among plots, ultrasonic test tones were broadcast at fixed distances (5–40 m), and sound attenuation was modeled to estimate effective detection distance[74]. Bat activity was then calculated at the plot level. Specifically, total call duration and number of detected calls were summed across tagged recordings and divided by the plot-specific detection area, yielding activity expressed as seconds per hectare and calls per hectare[75]. These standardized measures were used as indicators of bat activity in subsequent analyses.

Canopy and litter arthropods (ants, beetles, spiders and wasps)

Canopy arthropods were collected using canopy fogging between late June and early October 2021. In each plot, 50 mL DECIS 25 EC (Bayer Crop Science, 25 g/L deltamethrine) mixed in four liters of petroleum oil were applied to the canopy at the center of each plot using a Swingfog SN50 (Swingtec, Isny, Germany). Underneath the canopy, ten conical collection traps measuring 1 m × 1 m were placed. Each trap was fitted with a 250 mL polyethylene bottle filled with 100 mL of 96% ethanol. Two hours after application of the insecticide, the ten polyethylene bottles of each plot were removed, combined into a single sample, and stored at -20°C. More details on the fogging method are available in Pollierer et al[76].

Leaf litter arthropods were collected alongside canopy fogging from four 1 m × 1 m subplots. Litter and small deadwood within frames were collected, coarsely minced and placed in a 4 mm mesh inlet sack into Winkler extractors. Each extractor was fitted with a 250 mL polyethylene bottle tied to the bottom, containing 100 mL 96% ethanol. Winkler extraction ran for 48 h, and inlet sacks were gently shaken after the first 24 hours. The four polyethylene bottles of each plot were combined into a single sample and stored at -20°C.

256,475 arthropod specimens were collected with canopy fogging in 125 of 128 EFForTS-LA plots, and 149,228 specimens were collected from leaf litter from 116 of 128 plots (not all plots were accessible for leaf litter collection due to flooding). Samples were sorted to orders, and ants, beetles, spiders and wasps identified at high taxonomic level. In ants, 67,655 workers from the canopy were sorted to 46 genera and 56,687 workers from leaf litter to 78 genera. Beetles are represented by the four numerically dominant families Curculionidae (weevils), Chrysomelidae (leaf beetles), Elateridae (click beetles) and Staphylinidae (rove beetles), which together contribute more than half of the overall beetle fauna from an earlier campaign[61]. In beetles, 13,208 specimens from the canopy were sorted to 149 genera and 26 subfamilies (when genus was unknown), and 3350 from the leaf litter to 58 genera and 18 subfamilies. In spiders, 11,380 specimens from the canopy were sorted to 220 genera and 23 morphogenera (subdivisions on family level with unknown genus), and 1238 specimens from the leaf litter to 123 genera and 18 morphogenera. Wasps are represented by the family Scelionidae, which were the second most abundant of 30 families in overall 13,295 hymenopteran parasitoids; 1331 Scelionids from the canopy were sorted to 184 morphospecies and 321 specimens from the leaf litter to 89 morphospecies. Ants, beetles and spiders are documented on Ecotaxonomy.org and in Nazarreta et al., Hidayat et al. and Dhiya'ulhaq et al[77–79].

Soil fauna

For each plot, from each of the four subplots, one randomly positioned soil core sample was taken. Each core measured 10 cm in diameter and included litter and soil to a depth of 5 cm. Litter and soil layer were separated in the field and extracted independently. Samples were transported to the laboratory for extraction of soil animals. Animals were extracted by Tullgren extractor, with the four subplot samples from the same plot extracted together. Animals were collected in 96% ethanol and frozen until further

transportation and processing. Animals were sorted to group level, and Collembola were further determined to species or morphological species level under a dissecting microscope (Stemi 508, Zeiss, Jena, Germany) at 50x magnification based on morphological characters (body shape, morphology of furca, antennae, number of eyes). A maximum of 10 individuals of each morphological group from each sample were subsequently cleared with Nesbitt solution on a heating plate (50°C for 3-10 min. Collembola were then identified to species or morphospecies level using a compound microscope (Axiovert 35, Zeiss) at maximum 400x magnification using the checklist for Indonesian Collembola and additional articles containing keys for Collembola of southeast Asia, particularly Indonesia[80,81]. In total, across all land-use systems 7,870 soil and litter Collembola individuals were assigned to 64 species from 46 genera and 16 families.

Field sampling for DNA extraction for microbial community and nematodes

Field sampling was conducted from May 2021 to August 2022 across plots in forest, shrubland, rubber, and oil palm systems. At each plot, five soil cores were collected to a depth of 10 cm using a 5 cm diameter steel corer. Litter and soil were separated in the field with DNA-free tools and placed into labeled plastic bags. Samples were transported on ice to the field facility and processed immediately. Samples were divided into three compartments: litter, bulk soil, and roots (fine roots with adhering soil, representing the rhizosphere). Litter (50–400 g fresh weight per plot) was cut into ~1 cm pieces and manually homogenized. Soil (~1 kg per plot) was homogenized and sieved through 5mm and 1 mm mesh to remove roots; the sieved fraction was designated as bulk soil, roots were manually separated, blotted dry, and weighed. Subsamples (10 g litter, 15 g soil, and all recovered roots) were frozen overnight at −80 °C and lyophilized using a VirTis BenchTop K system (SP Industries, Warminster, USA) at the University of Jambi, Indonesia. All dried material was subsequently stored on silica gel. Aliquots (~100 mg roots, 250 mg soil, 150 mg litter) were used for DNA extraction. Root DNA was extracted with the InnuPREP Plant Kit (Analytik Jena AG, Germany), while soil and litter DNA were extracted using the DNeasy PowerSoil Kit (Qiagen, Germany).

Bacteria

Bacterial community was investigated through amplification of 16S rRNA gene using universal eubacteria primer set that target V3–V4 region[82] to 372 of total genomic DNA, extracted from bulk soil, litter, and rhizosphere. For each DNA sample, polymerase chain reaction (PCR) was performed in three replications and the amplicons generated were pooled for purification using MagSi-NGSPREP Plus. Purified amplicons were randomized on sequencing plates along with amplicons from the mock community (ZymoBIOMICS,USA) which acted as a positive control. Amplicon sequencing was performed by The Gottingen Genomics Laboratory using Illumina MiSeq platform. Raw reads were analyzed using the ngs4ecoprod ngs4_16S pipeline (https://github.com/dschnei1/ngs4ecoprod). For quality control, fastp 0.23.4 program[83] was employed to filter and trim the reads with a Phred score of 20 and sliding window of 4. Primer's removals were performed by cutadapt 4.4[84]. These paired end reads were merged and size filtered applying ≥400 bp as threshold using VSEARCH v2.23[85]. Chimera removal was

conducted de novo as well as aligned them against the SILVA 138.1 database. Reads were mapped back against the SILVA 138.1 database using BLASTn megablast 2.14.1+. For taxon classification, percentage similarity of <98.7 for species, <94.5 for genus, <86.5 for family, <82.0 for order, <78.5 for class, and <75 for phylum was set as threshold[86].

Fungi

The ITS2 region was amplified using the the primer pair ITS3-KYO2 and ITS4[87]. PCR reactions contained 5 µl DNA (7 ng μl^{-1}), 0.3 µl Phusion High-Fidelity DNA Polymerase (2 U μl^{-1}), 6 µl 5×Phusion HF Buffer, 0.6 µl of each primer (10 µM), 0.09 µl $MgCl_2$ (50 mM), and 0.6 µl dNTPs (10 mM), with nuclease-free water added to a final volume of 30 µl. Thermal cycling consisted of an initial denaturation at 98 °C for 1 min, followed by 25 cycles of denaturation at 98 °C for 45 s, annealing at 48 °C for 45 s, and extension at 72 °C for 30 s. PCR products were purified using MagSi-NGSPrep Plus magnetic beads (MagnaMedics GmbH, Aachen, Germany) to isolate the expected ~400 bp fragment. Amplicon sequencing was performed on the Illumina MiSeq platform using the MiSeq Reagent Kit v3 (Illumina Inc., San Diego, USA).

Raw paired reads were clipped by cutadapt v.4.5 to remove primers[84]. Then, low quality reads were filtered by fastp v.0.23.2 and reads ≥120 bp were retained[83]. Subsequently, filtered reads were merged using pear v0.9.11 with a minimum of five overlapping bases[88]. VSEARCH v2.15.2 was used for exclusion of reads shorter than 140 bp and longer than 600 bp[85]. The remaining reads were dereplicated, denoised and screened for chimeras against the UNITE v.8.97 public database to generate an ASV library[89]. Finally, filtered reads were mapped to the ASV library to generate the abundance table with 97% genetic identity. ASVs were identified using the BLAST algorithm against the UNITE database; only ASVs assigned to the fungal kingdom were retained in the table. In total, we obtained 24 million fungal reads and 39,321 ASVs across 377 samples. Samples with fewer than 600 total ASV counts and ASVs represented by fewer than 35 counts per sample were removed, 10,717 fungal ASV across 375 samples. Fungal richness was quantified as the number of ASVs detected per sample.

Protists

Protist communities were characterized by amplifying the V4 region of the 18S rRNA gene using the general eukaryotic primers TAReuk454FWD1 and TAReukREV3[90], with Illumina adapter overhangs, followed by paired-end sequencing on an Illumina MiSeq platform[91]. Raw reads were quality-filtered using fastp[83] with a minimum per-base Phred score of 20, sliding-window trimming (window size = 4, mean quality = 20), overlap-based base correction, and a minimum read length of 250 bp. Reads were merged, and primer sequences were removed using cutadapt[84]. After paired-end read merging, amplicon sequences were sorted by length and filtered to retain sequences ≥350 bp, corresponding to the expected size of the targeted 18S rRNA gene V4 region, and subsequently dereplicated using VSEARCH (--derep_fulllength). ASVs were inferred using UNOISE3 implemented in VSEARCH[85] with a minimum abundance threshold of 8, and chimeras were removed using both de novo and reference-based

methods against the SILVA database (v138.1). After excluding singletons/doubletons and non-protist sequences, a total of 3,616 protist ASVs were retained for downstream analyses.

Nematode

The hypervariable V4 region of the 18S rRNA gene was targeted in this study. Amplicons were generated following the semi-nested PCR protocol[92,93]. Briefly, an initial pre-amplification was performed using primers NemF and 18Sr2b, followed by a semi-nested PCR using primers NF1 and 18Sr2b. For Illumina MiSeq sequencing, the gene-specific primers NF1 and 18Sr2b were each fused to Illumina Nextera XT adapter overhang sequences, with the forward and the reverse overhang. During sequence processing, adapter and primer sequences were removed prior to quality filtering. Reads with a minimum quality score below Q20 or a final length shorter than 50 bp were discarded. To minimize the inclusion of non-specific amplification products, only sequences matching the expected 18S rRNA gene V4 amplicon length (250 bp) were retained for downstream analyses. Samples with fewer than 1000 total reads were removed and a total of 3,817 nematode ASVs across 305 samples were retained for downstream analyses.

Trees

All alive trees within each plot that had a diameter at breast height (dbh) ≥ 10 cm were censused. Each tree was given a preliminary field name and for each field name in each plot, one individual was selected for the recording of field photographs and collection of a herbarium specimen for later species identification. Two duplicates were collected from sterile individuals and up to eight from flowering and/or fruiting trees. Specimens were dried and pressed and distributed to herbaria in Indonesia (BIOT, BO, herbarium of the University of Jambi) and Germany (GOET, herbarium acronyms follow Index Herbariorum: https://sweetgum.nybg.org/science/ih/). Tree richness was calculated as the number of tree species per plot.

Pollen

Pollen traps were installed in each of the 62 core plots representing natural rainforest, shrubland and two agroforest management systems (rubber, and oil palm plantations) in the Bukit Duabelas (BD) and Harapan (HR) regions, Batanghari main region, Pematang Kabau and REKI. The traps followed the design of Behling pollen traps[94] and consisted of a hard plastic tube placed on the ground containing a test tube filled with synthetic cotton, approximately 5 ml of glycerol, and covered by a mosquito net and an external metal net. Pollen and spores were retained in the glycerol-soaked cotton, preventing washout due to precipitation. Traps were installed and retrieved annually in September and remained in the field for one year.

Samples were processed following standard laboratory procedures[95]. After sieving (1–2 mm), two Lycopodium tablets were added to estimate pollen concentration. Carbonates were removed using 10% HCl, followed by dehydration, acetolysis, and fine sieving (200 µm). Slides were prepared with glycerine

wax. Samples were counted to 300 pollen grains per plot, identified to the lowest possible taxonomic level, and expressed as percentages of the total pollen sum.

Root and Litter metabarcoding

Roots mixed with soil and litter were collected using five soil cylinder cores measuring 5 cm in diameter and 10 cm in depth, taken from the four corners of each subplot and one from the center. Samples were placed in cooling containers at the time of collection and subsequently stored at 4 °C until further processing. The cores were then pooled and homogenized, with one composite sample generated per plot. Root samples were dried using a freeze dryer (Alpha 1–2 LDplus) for 24–48 h. Root weight was recorded before and after drying for biomass calculations. Fine roots were shredded using a RETSCH Mixer Mill MM 400 at 30 Hz for 20–30 s until powdered, while processed in liquid nitrogen. DNA from fine roots was extracted using the innuPREP Plant DNA Extraction Kit (Innuscreen GmbH). Templates of mixed roots from each plot were amplified targeting the ribulose-1,5-bisphosphate carboxylase large chain (*rbcL*) region using primers rbcL2 and rbcLa in triplicate PCR reactions. Positive and negative controls were included in all steps. Remaining reagents were removed using the GENECLEAN Kit (MP Biomedicals). Sample concentrations were measured with a Qubit fluorescence spectrophotometer (Life Technologies) and standardized to 200 ng per sample. Sequencing libraries were prepared using the Illumina TruSeq Nano DNA High Throughput Library Prep Kit (96 samples) and Illumina TruSeq DNA CD Indexes. Details of the DNA metabarcoding approach and the bioinformatic pipeline implemented are described in Moura et al.[96]. Paired-end sequencing was performed on an Illumina MiSeq platform using the MiSeq Reagent Kit v2 (300 cycles), with DNA libraries loaded at 10 pM and 10% PhiX control, at the NGS Integrative Genomics Core Unit (NIG), University of Göttingen.

In addition, litter samples were collected by separating the upper litter layer from each of the five soil cores per subplot into litter and soil fractions for plant identification using DNA metabarcoding using a similar protocol implemented for root samples. All litter material from the five cores was pooled into a single bag, resulting in one litter sample per plot. Litter samples were placed in cooling boxes immediately after collection and transported to the laboratory. Litter samples were first rinsed and cleaned to remove contaminants. A homogenized aliquot of the cleaned material was then centrifuged at 11,000 rpm for 1 min, followed by washing with nuclease-free water. The supernatant was discarded, and this procedure was repeated twice using 1,000 µl of ethanol for each wash. A final rinse with nuclease-free water was performed, and the processed samples were transferred to Lysis Tubes Z (Analytik Jena AG) for DNA extraction. DNA was isolated using the Plant DNA Extraction Kit (Analytik Jena AG), following the manufacturer's protocol. Litter DNA was also amplified targeting the rbcL region. The primers rbcL2 and rbcla-R were used, generating PCR products of approximately 450 bp. To ensure reliable detection of plant species with low DNA concentrations, triplicate PCRs were also performed. Subsequent processing of the samples followed the same procedures as described above for root DNA. Sequencing and bioinformatic analysis are detailed in Moura et al.[96].

Ecosystem function indices

Predation

Predation rates were quantified using artificial caterpillar mimics made from green plasticine (Pelikan Nakiplast®, 35 × 5 mm), following widely applied protocols for estimating predation pressure in tropical agroecosystems[97,98]. At each study plot, 36 dummy caterpillars were deployed across four subplots located 12 m from the plot center in the four cardinal directions, with nine caterpillars arranged in a 3 × 3 m grid per subplot. Dummies were attached to the mid-veins of intact leaves at approximately 1 m height in the understory vegetation using insect pins. In the absence of understory vegetation (e.g., in oil palm or shrubland subjected to regular weeding), dummies were placed directly on the ground. After 48 h of exposure, caterpillars were retrieved and inspected for predator bite marks. For each dummy, predation occurrence and predator identity were determined based on characteristic bite marks using published identification guides and photographic references[99]. Unknown but distinct bite marks were classified as morphotypes. Plot-level predation metrics were calculated from aggregated dummy-level observations. Predation rate was defined as the proportion of caterpillars showing bite marks relative to the total number of retrieved dummies.

Energy flux

We used a multichannel food web reconstruction method[100] and generated predator-prey adjacency matrices based on animal traits. These traits include feeding preferences, body mass, biomass, and protection traits. These traits were used to estimate the interaction probability among food web nodes. The following assumptions were used for the soil food web reconstruction[100]: (1) there are phylogenetically inherited differences in feeding preferences for various basal resources and predation capability among soil animal taxa, which define their feeding interactions; (2) predator-prey interactions are primarily defined by the optimum predator-prey mass ratio (PPMR, we assumed an optimum PPMR of 100). Typically, a predator is larger than its prey, but certain predator traits (e.g., hunting traits and behavior, parasitic lifestyle) can considerably modify the optimum PPMR; (3) predation is biomass-dependent. Due to a higher encounter rate, predators will preferentially feed on prey that is locally abundant; (4) the strength of the trophic interaction between a predator and a prey can be considerably reduced by prey protective traits. Each of the assumptions is used to produce a plausible interaction matrix, with all matrices finally multiplied together to obtain the food web topology.

Energy fluxes were calculated using the R package fluxweb[101], combining the food web matrices and the metabolic rates and assimilation efficiencies of each group. Metabolic rates were calculated based on average fresh body masses using the coefficients for the corresponding phylogenetic group of invertebrates[102] and the mean temperature of each land-use type. Diet-specific assimilation efficiencies were calculated based on the nitrogen content of each basal resource or prey[103]. To infer ecological functions, we calculated bulk parameters for each food web and classified energy fluxes according to

the basal resources/prey: canopy and litter herbivory, canopy and litter predation, litter bacterivory and fungivory, and litter transformation.

Aboveground biomass

Aboveground tree biomass (AGB) was obtained from measuring all trees inside the circular plots with a diameter at breast height (DBH) ≥10 cm. Tree height of living trees was recorded using a Vertex III height meter (Haglöf, Långsele, Sweden), and measuring tapes (Richter Measuring Tools, Speichersdorf, Germany) used for the diameter. Oil palm stem height was defined as the length from the base of the trunk to the uppermost base of the oil palm fronts. Wood density for each tree was estimated using the relationship between wood density values obtained from increment cores with penetration depth measured using a Pilodyn 6J Forest wood tester (PROCEQ, Zurich, Switzerland)[104]. Aboveground tree biomass AGB was calculated using the BIOMASS package[105] following the allometric equations of Chave et al. for trees[106], and Khasanah et al. for oil palms[107]. The individual tree AGB estimates were summed and areal normalized to Megagram per hectare.

Root biomass

Samples were collected between May 2021 and August 2022 using a cylindrical steel corer (5 cm in diameter) to a depth of 10 cm. Five cores were taken per plot. All samples were transported on ice to the field facility and processed immediately. Roots were washed, separated into fine and coarse roots (fine roots: < 2 mm diameter; coarse roots: ≥ 2 mm diameter), and weighed for fresh mass. Aliquots of fine roots and soil samples were immediately freeze-dried (Alpha 1-2 LDplus) for 24 to 48 hours and exported to the University of Göttingen (Germany) for molecular analysis. Fine-root biomass and coarse-root biomass were calculated separately as dry mass per unit ground area. For each root fraction, total fresh mass from the five cores was converted to dry mass using the dry-to-fresh mass ratio determined from the corresponding dried aliquot. The resulting dry mass was then divided by the total sampled area of the five soil cores and expressed as g m^{-2} [108].

Resistance to alien plant invasion

To estimate resistance to alien plant invasion, all aboveground living vascular plant mass within three 1m x 1m biomass squares in subplots A, B and C was sampled, harvested, and later weighted. These squares were positioned 1 m north of the center of each subplot. Plant material was separated into alien and native species, oven-dried at 70°C over 48 hours and weighed afterwards. The relative aboveground alien biomass (AGB alien/AGB alien + AGB native) was calculated and 1 - relative aboveground alien biomass was used as a proxy for resistance to alien plant invasion.

Leaf-gas exchange

Photosynthetic capacity (light-saturated photosynthetic rate, A_{sat}) was measured in the Landscape Assessment plots using a portable infrared gas exchange system (LI-6800, LI-COR BioSciences, Lincoln,

USA) with a 3 × 3 cm^2 leaf chamber from May 2021 to May 2022. Branches from the upper canopy of dominant tree species or palms were collected daily around 8 a.m. using big-shot or pruners and recut under water. Measurements were conducted on three fully expanded, mature leaves per branch.

Net photosynthesis (A_{net}) was measured at leaf temperatures of 28-45 °C, relative humidity of 20-81%, and a constant CO_2 concentration of 400 µmol mol^{-1}. Light-response curves were generated by stepwise reductions in photosynthetically active radiation from 2200 to 0 µmol photon m^{-2} s^{-1}, and A_{sat} was derived using a non-rectangular hyperbola model.

Microclimate stability

Microclimate measurements were collected from May to November 2021 using mini-meteorological stations equipped with a ClimaVUE 50 weather sensor (Campbell Scientific, Inc., Logan, USA) and two TRIME-PICO32 soil probes (IMKO GmbH., Ettlingen, Germany). The weather sensor mounted 2 m above ground, recorded air temperature (°C), relative humidity (%), air and vapour pressure (hPa), wind speed (m s^{-1}) and direction (° from North), solar radiation (W m^{-2}), and precipitation (mm). Soil moisture (%) and temperature (°C) were measured at 30 cm depth. Measurements were taken every 15 s, averaged to 1-min intervals, and stored on a CR300 data logger (Campbell Scientific, Inc., Logan, USA).

We partitioned the study area into 16 micro-regions, each roughly 4 km in radius and encompassing several land-use types, yielding a total of 118 measurement plots. Within each micro-region, four below-canopy weather stations simultaneously captured microclimatic conditions across land-use types, while one centrally located open-area station recorded background meteorology. Plot-level stations measured for 36–40 hours before being moved to the next plot, whereas the open-area station operated continuously until all plots in that micro-region were completed. After finishing a micro-region, the open-area station was relocated, and a new round of below-canopy measurements began. At each plot, we also collected instant near-surface soil moisture and temperature readings using a mobile Bluetooth soil sensor (IMKO PICO-BT, IMKO GmbH., Ettlingen, Germany).

To quantify short-term temporal microclimatic stability at the plot level, we derived stability indices for air temperature, relative humidity, soil temperature, and soil moisture from the summary statistics provided by the micro-meteorological stations. For each variable, stability was calculated as the ratio between the temporal mean and the corresponding standard deviation recorded during the 36–40 h measurement period at each plot. This index represents the inverse of temporal variability and provides a dimensionless proxy for microclimatic stability, where higher values indicate more stable conditions (i.e. lower relative fluctuations). Stability metrics were calculated separately for aboveground (air temperature and relative humidity) and belowground (soil temperature and soil moisture) environments and subsequently used as predictors in statistical analyses.

Litter decomposition

Litterbags (20 × 20 cm, 4 mm mesh size) containing 10 g dry leaf litter were incubated in situ in each study plot for six months (April–May to October–November 2021). One litterbag was placed in each plot. The litter used in the experiment consisted of representative plant material from the respective land-use systems. Rainforest litter comprised a mixture of freshly fallen leaves collected from a single forest plot, including 4 g *Terminalia bellirica*, 4 g *Endospermum diadenum* and 2 g *Alactonia* sp. Litter from rubber (*Hevea brasiliensis*) and oil palm (*Elaeis guineensis*) plantations was collected from the corresponding study sites and consisted of freshly fallen leaves in rubber and freshly cut fronds in oil palm[36]. Shrubland litter comprised a mixture of air-dried fresh leaves of *Clidemia hirta* and *Dicranopteris linearis* (5 g each). Litter mass loss was calculated as the difference between initial dry mass and dry mass remaining after six months and expressed as percentage of the initial litter mass.

Soil basal respiration and microbial biomass

Basal respiration (µl O2 g^{-1} h^{-1}) and microbial biomass (Cmic; µg g^{-1} dry weight) were determined by measuring O2 consumption using an automated respirometer system[109]. Prior to measurement, 3 g of soil and 0.5 g of litter (dry weight equivalent) were placed in sample vessels overnight at room temperature (20 °C). O_2 consumption was measured at 22 °C, with microbial CO_2 absorbed in alkaline solution and O_2 continuously replenished via electrolytic production. Basal respiration was calculated as the mean O_2 consumption once the system reached stable O_2 consumption. Microbial biomass was determined from the maximum initial respiratory response following glucose addition to saturate microbial glycolytic activity, and microbial biomass carbon was estimated using an established conversion factor[110]. Microbial specific respiration was calculated as the ratio of basal respiration to microbial biomass. Detailed protocols followed established procedures for substrate-induced respiration and oxygen micro-respirometry[109,111].

Leaf area index

Leaf Area Index (LAI) was assessed using a LAI-2200C Plant Canopy analyzer (LI-COR, Biosciences Inc., Lincoln, USA). We used two wands with optical sensors. One was positioned in an open area near the respective study plot, while simultaneously on the plot, data collection was conducted at all five sub-plots at a height of 1.3 m with the below-canopy wand. Measurements were obtained in the early morning before bright sunlight between June 2021 and March 2022.

Landscape metric calculation

To quantify landscape structure, we distinguished two categories of metrics: (i) landscape heterogeneity and (ii) the amount of natural habitat. Landscape heterogeneity was further divided into compositional heterogeneity, represented by land-use Shannon diversity, and configurational heterogeneity, represented by edge density. The amount of natural habitat was quantified as the percentage of forest cover within the surrounding landscape. For each study plot, metrics were calculated within circular buffers of eight

radii (100, 250, 500, 750, 1000, 1500, 2000, and 3000 m). Different land-use maps were employed depending on spatial scale to ensure the highest possible accuracy: Sentinel-based land-use maps were used for the largest buffer sizes (1500, 2000, and 3000 m); land-use maps derived from airborne LiDAR data[112] were used for intermediate buffer sizes (750 and 1000 m); and manually classified land-use maps based on airborne orthophotos were applied for fine-scale buffers (≤500 m).

All metrics were consistently computed using the R package *landscapemetrics*[113]. To validate the comparability of metrics derived from different map sources, we performed correlation analyses between edge density and Shannon diversity across the three map scales at 100, 250, and 500 m buffer scales, using the manually classified maps as a reference. Metrics from different maps were correlated, and correlations improved with increasing buffer size, supporting the robustness of our approach (Fig. S12).

Calculation of multidiversity and multifunctionality

Biodiversity was assessed across animals, microbes, and plants using taxonomic richness as a unifying metric with 34 indicators of 19 taxa from different microhabitats. Animal diversity comprised ants (canopy and belowground), arthropods, collembolans (litter and soil), spiders (canopy and belowground), nematodes (litter, soil, and rhizosphere), canopy beetles (click, leaf, weevil, rove), litter beetles (weevil, rove), wasps (canopy and belowground), as well as birds and bats (with activity used as a proxy for the latter). Microbial diversity was derived for fungi, protozoa, and bacteria from soil, litter and rhizosphere. Plant diversity included pollen, litter-associated taxa, roots-associated taxa, and tree species richness. Soil fungi, bacteria, protozoa, and nematodes from soil, litter, and root compartments were analyzed by DNA-based marker gene sequencing as amplicon sequence variants or OTUs, respectively. Hereafter, we refer to these different taxonomic units (species, morphotypes, genus, and OTU) as ‘species’ for simplicity. Other taxonomic groups were sorted to the lowest possible level (species or morphospecies), but some groups such as spiders, ants, and beetles were identified to the genus level. All indicators were standardized prior to analysis to allow comparability across groups and subsequently aggregated into multidiversity indices.

We quantified ecosystem functioning using 20 indicators that capture complementary aspects of above- and belowground processes. Aboveground functions included predation rate, resistance to invasion (biomass of invasive species), aboveground biomass, canopy herbivory and predation, microclimatic variables (air temperature and humidity), and photosynthetic capacity of dominant tree species. Belowground functions comprised herbivory and predation by soil and litter fauna, soil microclimate (temperature and moisture), decomposition rate, litter transformation, basal respiration (litter and soil), microbial biomass (litter and soil), and root biomass (fine and coarse roots). Together, these variables reflect ecosystem processes related to productivity, resistance to biotic stress, trophic interactions, carbon and nutrient cycling, and microclimate regulation. Prior to index construction, we screened the candidate functioning indicators for redundancy by inspecting pairwise Spearman rank correlations and

their influence on composite scores. Overall, correlations were low, indicating no pervasive collinearity across the indicator set; however, a small number of near-duplicate metrics were excluded to minimize double counting and improve interpretability of multifunctionality estimates.

To integrate biodiversity and ecosystem functions, we calculated multidiversity and multifunctionality by aggregating standardized indicators into composite indices[17,18]. Both metrics were derived using two approaches: (i) an averaging method, in which all standardized indicators were averaged to obtain a single value per plot, and (ii) a threshold method, in which the number of indicators exceeding a given proportion (25%, 50%, 75%) of their maximum observed value across all plots was counted[17]. To avoid redundancy in the main text, we present results based on the averaging method, while threshold-based results are provided in the Supplementary Information. Multidiversity and multifunctionality were calculated separately for aboveground and belowground indicators, as well as combined into an overall index. Given the larger number of belowground indicators, we additionally tested an alternative calculation of overall indices as the mean of aboveground and belowground values but results closely resembled those obtained from direct overall calculations.

Multidiversity was calculated separately for major organismal groups (animals, microbes, plants) and for different microhabitats (soil, litter, roots, canopy), in addition to aboveground, belowground, and overall multidiversity indices. Specifically, animal multidiversity comprised ants, arthropods, collembolans, spiders, beetles (click, leaf, weevil, rove), nematodes, wasps, birds, and bats; microbial multidiversity comprised fungi, protozoa, and bacteria across soil, litter, and root compartments; and plant multidiversity comprised pollen, litter-associated taxa, roots-associated taxa, and trees. Microhabitat-level multidiversity was calculated by grouping indicators by their primary habitat (soil, litter, roots, canopy).

Multifunctionality was quantified both as an overall index and within specific functional domains. Functional domains included (i) productivity (aboveground biomass, fine- and coarse-root biomass, saturated photosynthesis, and leaf area index), (ii) nutrient cycling (decomposition, litter transformation, basal respiration in litter and soil, and microbial biomass in litter and soil), (iii) energy fluxes (predator attack rate estimated using artificial caterpillars, as well as herbivory and predation energy fluxes in canopy and belowground compartments), and (iv) resistance and stability (biotic resistance to invasion based on plant biomass, and abiotic stability indicators of air temperature, air humidity, soil temperature, and soil moisture).

All calculations were conducted in R using standardized protocols[114].

Statistical analysis

We analyzed each biodiversity and functional indicator, multidiversity and ecosystem multifunctionality responses to local land-use types, and multidiversity and ecosystem multifunctionality responses to

landscape-scale variables based on the following framework. All statistical analyses were conducted in R version 4.5.1[114], using the packages *lme4*, *emmeans*, *multcomp*, and *bestNormalize*[115–118].

Local land-use effects on individual biodiversity and functional indicators

To test the effects of local land use on individual biodiversity and functional indices, we first excluded shrubland from the dataset and contrasted rainforests with plantations (rubber and oil palm combined). We fitted linear mixed-effects models (*lmer*) with standardized values (z-scores) of each indicator as the response, land-use type (*Forest* vs *Plantation*) and indicator identity as fixed effects, and plot identity as a random intercept. Effect sizes of *Plantation vs Forest* were extracted using estimated marginal means (*emmeans*) with *Forest* as the reference. P-values were adjusted for multiple testing using the false discovery rate (FDR). To facilitate interpretation, standardized effect sizes were back-transformed into the original scale and expressed as percentage change relative to forest means.

Local land-use effects on multidiversity and multifunctionality

Multidiversity and multifunctionality were calculated using both the averaging approach and the threshold approach at 25%, 50%, and 75% quantiles. We fitted linear models (*lm*) with land-use type (rainforest, shrubland, rubber and oil palm plantations) as a fixed effect separately for each metric. Post-hoc pairwise comparisons were performed with *emmeans* using Sidak correction for multiple testing. Effect sizes were also calculated relative to forests.

Landscape effects on multidiversity and multifunctionality

To quantify landscape effects, we related multidiversity and multifunctionality indices to landscape heterogeneity (edge density, land-use Shannon diversity) across multiple spatial scales (100–3000 m). Prior to analysis, each response variable was normalized using the *bestNormalize* procedure, which automatically selects appropriate transformations (e.g., Box–Cox, Yeo–Johnson or rank-based transformations)[119,120] to improve normality and comparability. For each response–predictor pair, we fitted linear models including land-use type and its interaction with the landscape variable. Significance of terms was assessed by ANOVA, and P-values were corrected across tests using the FDR procedure[121]. Exploratory analyses revealed that interaction effects with edge density and land-use Shannon diversity were generally weak, except for plant multidiversity at the 25% threshold, so we primarily focused on main effects.

Because forest-cover effects varied among local land-use types, we fitted land-use-specific linear models relating multidiversity or multifunctionality to forest cover measured at each spatial scale. Response variables and forest-cover predictors were standardized before model fitting to obtain comparable standardized slopes. Statistical support for each forest-cover effect was assessed from the slope test, and P-values were corrected using the Benjamini–Hochberg FDR procedure across the eight spatial scales within each response variable and land-use type.

To specifically assess the influence of landscape heterogeneity (edge density and land-use Shannon diversity) independent of local land use, we first regressed each multidiversity and multifunctionality index against local land-use type and extracted model residuals[122]. These residuals, representing the component of multidiversity and multifunctionality that is independent of local land-use effects, were then modeled as a function of landscape variables at multiple spatial scales. Model performance (R^2) and significance were assessed for each response–predictor combination, and P-values were adjusted using FDR correction. For the main and statistically significant models, residuals were visually inspected to confirm homogeneity of variance and approximate normality.

Declarations

Data Availability:

https://doi.org/10.6084/m9.figshare.31940088

Code Availability:

https://doi.org/10.6084/m9.figshare.31940088

Acknowledgments

We sincerely appreciate the Ministry of Research and Technology of Indonesia (RISTEK), the Indonesian Institute of Sciences (LIPI), the Ministry of Forestry (PHKA) and Restoration Ecosystem Indonesia (PT REKI) for granting research permits. We also extend our gratitude to our colleagues and field assistants for their invaluable support during fieldwork and laboratory analyses. The EFForTS Landscape Assessment (EFForTS-LA) was funded by the Deutsche Forschungsgemeinschaft (DFG, German Research Foundation), project number 192626868, within the framework of the collaborative German-Indonesian research project CRC 990/EFForTS. Z.Z., C.W., and I.G. were funded by the Deutsche Forschungsgemeinschaft (DFG), project number 532858005. Additional funding was provided by the Deutsche Forschungsgemeinschaft (DFG) within the bundle of projects (PAK proposal) “Conversion of rainforest into rubber and oil palm plantations in Sumatra, Indonesia: Landscape-scale changes in biodiversity and ecosystem functioning, and restoration pathways”, projects 532858005 (I.G. and C.W.), 532846413 (S.S.), and 532868192 (A.K.). The EFForTS Landscape Assessment (EFForTS-LA) was designed and implemented by Kevin Darras, Ingo Grass and Catrin Westphal with input from the entire EFForTS consortium. We thank the Indonesian and German coordinators for their outstanding efforts in conducting the joint field campaign and data collection. The responsibilities included: Arne Wenzel (general scientific coordination), Christian Stiegler, Ashehad A. Ali, Erwin P. Sakti and Basri Bin Daeng Mattone (environmental processes), Fabian Brambach, Anton Potapov, Carina Carneiro de Melo Moura, Martyna Kotowska, Jochen Drescher, Dian Muh. Fauzan, Patrick Diaz (above-ground biota and

processes), Valentyna Krashevska and Leonarda Situmorang (below-ground biota and processes), Kibrom Sibhatu and Zulkifli Alamsyah (human dimensions), Michael Schlund and Stefan Erasmi (remote sensing), and Zheng Zhou (data management). For administration and logistic support, we thank Aiyen Tjoa and the entire EFForTS office team in Jambi, Indonesia.

Author Contributions Statement

Z.Z. performed the visualization and wrote the original draft. I.G. and C.W. supervised the study. C.W., S.S. and I.G. acquired funding. Z.Z., C.W., I.G., A.W., K.D., H.B., R.D., S.E., O.G., D.H., A.K., A.Pol., M.Q., T.Ts., K.W., H.K. and S.S. conceptualized the study. J.D., V.K., A.W., K.D., C.S., M.S., F.B., A.Pot., C.M., M.M.K., K.T.S. and A.A.A. developed the methodology. J.D., V.K., A.W., K.D., C.S., M.S., F.B., A.Pot., C.M., M.M.K., K.T.S., A.A.A., D.A., D.B., N.U.D., P.H., I., K., A.M., S.M., Y.M., R.N., M.N.R., I.Z.S., W.I.S., S.T., A.T., T.Tr. and E.Y. conducted the investigation and collected the data. All authors contributed to interpretation of the results and reviewed and edited the manuscript.

Competing Interests Statement

We declare no conflict of interest.

References

1. Pan, Y. *et al.* A Large and Persistent Carbon Sink in the World's Forests. *Science***333**, 988–993 (2011).
2. Barlow, J. *et al.* The future of hyperdiverse tropical ecosystems. *Nature***559**, 517–526 (2018).
3. Myers, N., Mittermeier, R. A., Mittermeier, C. G., Da Fonseca, G. A. B. & Kent, J. Biodiversity hotspots for conservation priorities. *Nature***403**, 853–858 (2000).
4. Vancutsem, C. *et al.* Long-term (1990–2019) monitoring of forest cover changes in the humid tropics. *Sci. Adv.***7**, eabe1603 (2021).
5. Bourgoin, C. *et al.* Human degradation of tropical moist forests is greater than previously estimated. *Nature***631**, 570–576 (2024).
6. Dirzo, R. & Raven, P. H. Global State of Biodiversity and Loss. *Annu. Rev. Environ. Resour.***28**, 137–167 (2003).
7. Barnes, A. D. *et al.* Consequences of tropical land use for multitrophic biodiversity and ecosystem functioning. *Nat Commun***5**, 5351 (2014).
8. Clough, Y. *et al.* Land-use choices follow profitability at the expense of ecological functions in Indonesian smallholder landscapes. *Nat Commun***7**, (2016).
9. Qaim, M., Sibhatu, K. T., Siregar, H. & Grass, I. Environmental, Economic, and Social Consequences of the Oil Palm Boom. *Annu. Rev. Resour. Econ.***12**, 321–344 (2020).
10. Gibson, L. *et al.* Primary forests are irreplaceable for sustaining tropical biodiversity. *Nature***478**, 378–381 (2011).

11. Edwards, D. P. *et al.* Conservation of Tropical Forests in the Anthropocene. *Current Biology***29**, R1008–R1020 (2019).
12. Sirami, C. *et al.* Increasing crop heterogeneity enhances multitrophic diversity across agricultural regions. *Proc. Natl. Acad. Sci. U.S.A.***116**, 16442–16447 (2019).
13. Priyadarshana, T. S. *et al.* Crop and landscape heterogeneity increase biodiversity in agricultural landscapes: A global review and meta-analysis. *Ecology Letters***27**, e14412 (2024).
14. IPBES, Brondizio, E., Diaz, S., Settele, J. & Ngo, H. T. *Global Assessment Report on Biodiversity and Ecosystem Services of the Intergovernmental Science-Policy Platform on Biodiversity and Ecosystem Services*. https://zenodo.org/doi/10.5281/zenodo.3831673 (2019) doi:10.5281/ZENODO.3831673.
15. Wezel, A. *et al.* Agroecological principles and elements and their implications for transitioning to sustainable food systems. A review. *Agron. Sustain. Dev.***40**, 40 (2020).
16. Hooper, D. U. *et al.* EFFECTS OF BIODIVERSITY ON ECOSYSTEM FUNCTIONING: A CONSENSUS OF CURRENT KNOWLEDGE. *Ecological Monographs***75**, 3–35 (2005).
17. Byrnes, J. E. K. *et al.* Investigating the relationship between biodiversity and ecosystem multifunctionality: challenges and solutions. *Methods Ecol Evol***5**, 111–124 (2014).
18. Hector, A. & Bagchi, R. Biodiversity and ecosystem multifunctionality. *Nature***448**, 188–190 (2007).
19. Le Provost, G. *et al.* Contrasting responses of above- and belowground diversity to multiple components of land-use intensity. *Nat Commun***12**, 3918 (2021).
20. Grass, I. *et al.* Trade-offs between multifunctionality and profit in tropical smallholder landscapes. *Nat Commun***11**, 1186 (2020).
21. Newbold, T. *et al.* Global effects of land use on biodiversity differ among functional groups. *Functional Ecology***34**, 684–693 (2020).
22. Berkelmann, D., Schneider, D., Meryandini, A. & Daniel, R. Unravelling the effects of tropical land use conversion on the soil microbiome. *Environmental Microbiome***15**, 5 (2020).
23. Turley, N. E., Bell-Dereske, L., Evans, S. E. & Brudvig, L. A. Agricultural land-use history and restoration impact soil microbial biodiversity. *Journal of Applied Ecology***57**, 852–863 (2020).
24. Drescher, J. *et al.* Ecological and socio-economic functions across tropical land use systems after rainforest conversion. *Philos T R Soc B***371**, (2016).
25. Bardgett, R. D. & van der Putten, W. H. Belowground biodiversity and ecosystem functioning. *Nature***515**, 505–511 (2014).
26. Zemp, D. C. *et al.* Tree islands enhance biodiversity and functioning in oil palm landscapes. *Nature***618**, 316–321 (2023).
27. Stokely, T. D. *et al.* Experimental evaluation of herbicide use on biodiversity, ecosystem services and timber production trade-offs in forest plantations. *Journal of Applied Ecology***59**, 52–66 (2022).
28. Wang, M.-Q. *et al.* Cascading effects of tree diversity loss on herbivore-parasitoid interactions. *Biological Conservation***311**, 111418 (2025).

29. Zhou, Z., Krashevska, V., Widyastuti, R., Scheu, S. & Potapov, A. Tropical land use alters functional diversity of soil food webs and leads to monopolization of the detrital energy channel. *eLife***11**, e75428 (2022).
30. Allen, K., Corre, M. D., Kurniawan, S., Utami, S. R. & Veldkamp, E. Spatial variability surpasses land-use change effects on soil biochemical properties of converted lowland landscapes in Sumatra, Indonesia. *Geoderma***284**, 42–50 (2016).
31. Malik, A. A. *et al.* Land use driven change in soil pH affects microbial carbon cycling processes. *Nat Commun***9**, 3591 (2018).
32. Li, Z.-P. *et al.* Human land use promotes range expansion of soil protists from temperate to subtropical regions in China. *Proc. Natl. Acad. Sci. U.S.A.***122**, e2413220122 (2025).
33. Ni, Y. *et al.* Soil pH determines bacterial distribution and assembly processes in natural mountain forests of eastern China. *Global Ecol. Biogeogr.***30**, 2164–2177 (2021).
34. Krause, A. *et al.* Quantifying the impacts of land cover change on gross primary productivity globally. *Sci Rep***12**, 18398 (2022).
35. Potapov, A. M. *et al.* Rainforest transformation reallocates energy from green to brown food webs. *Nature***627**, 116–122 (2024).
36. Krashevska, V. *et al.* Micro-decomposer communities and decomposition processes in tropical lowlands as affected by land use and litter type. *Oecologia***187**, 255–266 (2018).
37. Tscharntke, T., Klein, A. M., Kruess, A., Steffan-Dewenter, I. & Thies, C. Landscape perspectives on agricultural intensification and biodiversity – ecosystem service management. *Ecology Letters***8**, 857–874 (2005).
38. Leibold, M. A. *et al.* The metacommunity concept: a framework for multi-scale community ecology. *Ecology Letters***7**, 601–613 (2004).
39. Hass, A. L. *et al.* Landscape configurational heterogeneity by small-scale agriculture, not crop diversity, maintains pollinators and plant reproduction in western Europe. *Proc. R. Soc. B.***285**, 20172242 (2018).
40. Tscharntke, T., Grass, I., Wanger, T. C., Westphal, C. & Batáry, P. Beyond organic farming – harnessing biodiversity-friendly landscapes. *Trends in Ecology & Evolution***36**, 919–930 (2021).
41. Balmford, A. Extinction filters and current resilience: the significance of past selection pressures for conservation biology. *Trends in Ecology & Evolution***11**, 193–196 (1996).
42. Betts, M. G. *et al.* Extinction filters mediate the global effects of habitat fragmentation on animals. *Science***366**, 1236–1239 (2019).
43. Schmitt, T. Molecular biogeography of Europe: Pleistocene cycles and postglacial trends. *Front Zool***4**, 11 (2007).
44. Andermann, T., Strömberg, C. A. E., Antonelli, A. & Silvestro, D. The origin and evolution of open habitats in North America inferred by Bayesian deep learning models. *Nat Commun***13**, 4833 (2022).

45. Hua, F. *et al.* Ecological filtering shapes the impacts of agricultural deforestation on biodiversity. *Nat Ecol Evol***8**, 251–266 (2024).
46. Pearce, E. A. *et al.* Substantial light woodland and open vegetation characterized the temperate forest biome before *Homo sapiens*. *Sci. Adv.***9**, eadi9135 (2023).
47. Shipley, J. R. *et al.* Agricultural practices and biodiversity: Conservation policies for semi-natural grasslands in Europe. *Current Biology***34**, R753–R761 (2024).
48. Perfecto, I. & Vandermeer, J. The agroecological matrix as alternative to the land-sparing/agriculture intensification model. *Proc. Natl. Acad. Sci. U.S.A.***107**, 5786–5791 (2010).
49. Benton, T. G., Vickery, J. A. & Wilson, J. D. Farmland biodiversity: is habitat heterogeneity the key? *Trends in Ecology & Evolution***18**, 182–188 (2003).
50. Fierer, N. & Jackson, R. B. The diversity and biogeography of soil bacterial communities. *Proc. Natl. Acad. Sci. U.S.A.***103**, 626–631 (2006).
51. Delgado-Baquerizo, M. *et al.* A global atlas of the dominant bacteria found in soil. *Science***359**, 320–325 (2018).
52. Ettema, C. Spatial soil ecology. *Trends in Ecology & Evolution***17**, 177–183 (2002).
53. Logue, J. B., Mouquet, N., Peter, H. & Hillebrand, H. Empirical approaches to metacommunities: a review and comparison with theory. *Trends in Ecology & Evolution***26**, 482–491 (2011).
54. Loreau, M. *et al.* Biodiversity and Ecosystem Functioning: Current Knowledge and Future Challenges. *Science***294**, 804–808 (2001).
55. Tilman, D., Isbell, F. & Cowles, J. M. Biodiversity and Ecosystem Functioning. *Annu. Rev. Ecol. Evol. Syst.***45**, 471–493 (2014).
56. Liu, J. *et al.* How does habitat fragmentation affect the biodiversity and ecosystem functioning relationship? *Landscape Ecol***33**, 341–352 (2018).
57. Thompson, P. L. & Gonzalez, A. Ecosystem multifunctionality in metacommunities. *Ecology***97**, 2867–2879 (2016).
58. Thies, C. & Tscharntke, T. Landscape Structure and Biological Control in Agroecosystems. *Science***285**, 893–895 (1999).
59. Malhi, Y., Gardner, T. A., Goldsmith, G. R., Silman, M. R. & Zelazowski, P. Tropical Forests in the Anthropocene. *Annu. Rev. Environ. Resour.***39**, 125–159 (2014).
60. Ramos, D. *et al.* Rainforest conversion to rubber and oil palm reduces abundance, biomass and diversity of canopy spiders. *PeerJ***10**, e13898 (2022).
61. Kasmiatun *et al.* Rainforest conversion to smallholder cash crops leads to varying declines of beetles (Coleoptera) on Sumatra. *Biotropica***55**, 119–131 (2023).
62. Azhar, A. *et al.* Rainforest conversion to cash crops reduces abundance, biomass and species richness of parasitoid wasps in Sumatra, Indonesia. *Agri and Forest Entomology***24**, 506–515 (2022).
63. Prabowo, W. E. *et al.* Bird Responses to Lowland Rainforest Conversion in Sumatran Smallholder Landscapes, Indonesia. *PLoS ONE***11**, e0154876 (2016).

64. Rizky Nazarreta *et al.* Rainforest conversion to smallholder plantations of rubber or oil palm leads to species loss and community shifts in canopy ants (Hymenoptera: Formicidae). https://doi.org/10.25849/MYRMECOL.NEWS_030:175 (2020) doi:10.25849/MYRMECOL.NEWS_030:175.
65. Steffan-Dewenter, I. *et al.* Tradeoffs between income, biodiversity, and ecosystem functioning during tropical rainforest conversion and agroforestry intensification. *Proc. Natl. Acad. Sci. U.S.A.***104**, 4973–4978 (2007).
66. Kleijn, D., Rundlöf, M., Scheper, J., Smith, H. G. & Tscharntke, T. Does conservation on farmland contribute to halting the biodiversity decline? *Trends in Ecology & Evolution***26**, 474–481 (2011).
67. Thompson, P. L. *et al.* A process-based metacommunity framework linking local and regional scale community ecology. *Ecology Letters***23**, 1314–1329 (2020).
68. Tscharntke, T. *et al.* Landscape moderation of biodiversity patterns and processes - eight hypotheses. *Biological Reviews***87**, 661–685 (2012).
69. Hanski, I. & Ovaskainen, O. The metapopulation capacity of a fragmented landscape. *Nature***404**, 755–758 (2000).
70. Gray, C. L., Simmons, B. I., Fayle, T. M., Mann, D. J. & Slade, E. M. Are riparian forest reserves sources of invertebrate biodiversity spillover and associated ecosystem functions in oil palm landscapes? *Biological Conservation***194**, 176–183 (2016).
71. Scriven, S. A., Beale, C. M., Benedick, S. & Hill, J. K. Barriers to dispersal of rain forest butterflies in tropical agricultural landscapes. *Biotropica***49**, 206–216 (2017).
72. Kahl, S., Wood, C. M., Eibl, M. & Klinck, H. BirdNET: A deep learning solution for avian diversity monitoring. *Ecological Informatics***61**, 101236 (2021).
73. Wood, C. M. & Kahl, S. Guidelines for appropriate use of BirdNET scores and other detector outputs. *J Ornithol***165**, 777–782 (2024).
74. Darras, K., Pütz, P., Fahrurrozi, Rembold, K. & Tscharntke, T. Measuring sound detection spaces for acoustic animal sampling and monitoring. *Biological Conservation***201**, 29–37 (2016).
75. Krings, C. H., Darras, K., Hass, A., Batáry, P. & Fabian, Y. Not only hedgerows, but also flower fields can enhance bat activity in intensively used agricultural landscapes. *Basic and Applied Ecology***63**, 23–35 (2022).
76. Pollierer, M. M. *et al.* Rainforest conversion to plantations fundamentally alters energy fluxes and functions in canopy arthropod food webs. *Ecology Letters***26**, 1663–1675 (2023).
77. Naufal Urfi Dhiya'ulhaq *et al.Spiders of Jambi: A Guide to the EFForTS Collection*. (Penerbit BRIN, 2024). doi:10.55981/brin.824.
78. Nazarreta, R. *et al.A Guide to the Ants of Jambi (Sumatra, Indonesia): Identification Key to Ant Genera and Images of the EFForTS Collection*. (Penerbit BRIN, 2021). doi:10.14203/press.273.
79. Purnama Hidayat *et al.Guidebook of Beetles and Weevils of Jambi, Sumatra, Indonesia (Chrysomelidae, Curculionidae, Elateridae, and Staphylinidae)*. (Penerbit BRIN, 2022).

doi:10.55981/brin.321.

80. Mateos, E. Towards understanding Lepidocyrtus Bourlet, 1839 (Collembola, Entomobryidae) I: diagnosis of the subgenus Setogaster, new records and redescriptions of species. *Zootaxa***4044**, (2015).
81. Susanti, W. I. *et al.* Conversion of rainforest into oil palm and rubber plantations affects the functional composition of litter and soil Collembola. *Ecology and Evolution***11**, 10686–10708 (2021).
82. Klindworth, A. *et al.* Evaluation of general 16S ribosomal RNA gene PCR primers for classical and next-generation sequencing-based diversity studies. *Nucleic Acids Research***41**, e1–e1 (2013).
83. Chen, S., Zhou, Y., Chen, Y. & Gu, J. fastp: an ultra-fast all-in-one FASTQ preprocessor. *Bioinformatics***34**, i884–i890 (2018).
84. Martin, M. Cutadapt removes adapter sequences from high-throughput sequencing reads. *EMBnet j.***17**, 10 (2011).
85. Rognes, T., Flouri, T., Nichols, B., Quince, C. & Mahé, F. VSEARCH: a versatile open source tool for metagenomics. *PeerJ***4**, e2584 (2016).
86. Yarza, P. *et al.* Uniting the classification of cultured and uncultured bacteria and archaea using 16S rRNA gene sequences. *Nat Rev Microbiol***12**, 635–645 (2014).
87. Toju, H., Tanabe, A. S., Yamamoto, S. & Sato, H. High-Coverage ITS Primers for the DNA-Based Identification of Ascomycetes and Basidiomycetes in Environmental Samples. *PLoS ONE***7**, e40863 (2012).
88. Zhang, J., Kobert, K., Flouri, T. & Stamatakis, A. PEAR: a fast and accurate Illumina Paired-End reAd mergeR. *Bioinformatics***30**, 614–620 (2014).
89. Kõljalg, U. *et al.* Towards a unified paradigm for sequence-based identification of fungi. *Molecular Ecology***22**, 5271–5277 (2013).
90. Stoeck, T. *et al.* Multiple marker parallel tag environmental DNA sequencing reveals a highly complex eukaryotic community in marine anoxic water. *Molecular Ecology***19**, 21–31 (2010).
91. Schulz, G. *et al.* Changes in Trophic Groups of Protists With Conversion of Rainforest Into Rubber and Oil Palm Plantations. *Front. Microbiol.***10**, 240 (2019).
92. Wang, S. *et al.* Optimising high-throughput sequencing data analysis, from gene database selection to the analysis of compositional data: a case study on tropical soil nematodes. *Front. Ecol. Evol.***12**, 1168288 (2024).
93. Sapkota, R. & Nicolaisen, M. High-throughput sequencing of nematode communities from total soil DNA extractions. *BMC Ecol***15**, 3 (2015).
94. Jantz, N., Homeier, J., León-Yánez, S., Moscoso, A. & Behling, H. Trapping pollen in the tropics — Comparing modern pollen rain spectra of different pollen traps and surface samples across Andean vegetation zones. *Review of Palaeobotany and Palynology***193**, 57–69 (2013).
95. Fægri, K., Iversen, J., Kaland, P. E. & Krzywinski, K. *Textbook of Pollen Analysis*. (Blackburn Press, Caldwell, NJ, 2007).

96. Carneiro De Melo Moura, C. *et al.* Land-use changes impact root–fungal network connectivity in a global biodiversity hotspot. *Journal of Ecology***113**, 1136–1149 (2025).
97. Schwab, D. *et al.* Decreasing predation rates and shifting predator compositions along a land-use gradient in Madagascar's vanilla landscapes. *Journal of Applied Ecology***58**, 360–371 (2021).
98. Maas, B., Tscharntke, T., Saleh, S., Dwi Putra, D. & Clough, Y. Avian species identity drives predation success in tropical cacao agroforestry. *Journal of Applied Ecology***52**, 735–743 (2015).
99. Nurdiansyah, F., Denmead, L. H., Clough, Y., Wiegand, K. & Tscharntke, T. Biological control in Indonesian oil palm potentially enhanced by landscape context. *Agriculture, Ecosystems & Environment***232**, 141–149 (2016).
100. Potapov, A. M. Multifunctionality of belowground food webs: resource, size and spatial energy channels. *Biological Reviews* brv.12857 (2022) doi:10.1111/brv.12857.
101. Gauzens, B. *et al.fluxweb* : An R package to easily estimate energy fluxes in food webs. *Methods Ecol Evol***10**, 270–279 (2019).
102. Ehnes, R. B., Rall, B. C. & Brose, U. Phylogenetic grouping, curvature and metabolic scaling in terrestrial invertebrates: Invertebrate metabolism. *Ecology Letters***14**, 993–1000 (2011).
103. Jochum, M. *et al.* Decreasing Stoichiometric Resource Quality Drives Compensatory Feeding across Trophic Levels in Tropical Litter Invertebrate Communities. *The American Naturalist***190**, 131–143 (2017).
104. Kotowska, M. M., Hertel, D., Rajab, Y. A., Barus, H. & Schuldt, B. Patterns in hydraulic architecture from roots to branches in six tropical tree species from cacao agroforestry and their relation to wood density and stem growth. *Front. Plant Sci.***6**, (2015).
105. Réjou-Méchain, M., Tanguy, A., Piponiot, C., Chave, J. & Hérault, B. biomass : an r package for estimating above-ground biomass and its uncertainty in tropical forests. *Methods Ecol Evol***8**, 1163–1167 (2017).
106. Chave, J. *et al.* Improved allometric models to estimate the aboveground biomass of tropical trees. *Global Change Biology***20**, 3177–3190 (2014).
107. Khasanah, N., Van Noordwijk, M., Ningsih, H. & Rahayu, S. Carbon neutral? No change in mineral soil carbon stock under oil palm plantations derived from forest or non-forest in Indonesia. *Agriculture, Ecosystems & Environment***211**, 195–206 (2015).
108. Ballauff, J. *et al.* Shifts in root and soil chemistry drive the assembly of belowground fungal communities in tropical land-use systems. *Soil Biology and Biochemistry***154**, 108140 (2021).
109. Scheu, S. Automated measurement of the respiratory response of soil microcompartments: Active microbial biomass in earthworm faeces. *Soil Biology and Biochemistry***24**, 1113–1118 (1992).
110. Beck, T. *et al.* An inter-laboratory comparison of ten different ways of measuring soil microbial biomass C. *Soil Biology and Biochemistry***29**, 1023–1032 (1997).
111. Anderson, J. P. E. & Domsch, K. H. A physiological method for the quantitative measurement of microbial biomass in soils. *Soil Biology and Biochemistry***10**, 215–221 (1978).

112. Camarretta, N. *et al.* Using Airborne Laser Scanning to Characterize Land-Use Systems in a Tropical Landscape Based on Vegetation Structural Metrics. *Remote Sensing***13**, 4794 (2021).
113. Hesselbarth, M. H. K., Sciaini, M., With, K. A., Wiegand, K. & Nowosad, J. *landscapemetrics* : an open-source *R* tool to calculate landscape metrics. *Ecography***42**, 1648–1657 (2019).
114. R Core Team. *R: A Language and Environment for Statistical Computing*. (R Foundation for Statistical Computing, Vienna, Austria, 2020).
115. Bates, D., Mächler, M., Bolker, B. & Walker, S. Fitting Linear Mixed-Effects Models Using lme4. *Journal of Statistical Software***67**, 1–48 (2015).
116. Lenth, R. V. *Emmeans: Estimated Marginal Means, Aka Least-Squares Means*. (2021).
117. Hothorn, T., Bretz, F. & Westfall, P. Simultaneous Inference in General Parametric Models. *Biometrical J***50**, 346–363 (2008).
118. Peterson, R., A. Finding Optimal Normalizing Transformations via bestNormalize. *The R Journal***13**, 310 (2021).
119. Box, G. E. P. & Cox, D. R. An Analysis of Transformations. *Journal of the Royal Statistical Society Series B: Statistical Methodology***26**, 211–243 (1964).
120. Yeo, I.-K. A new family of power transformations to improve normality or symmetry. *Biometrika***87**, 954–959 (2000).
121. Benjamini, Y. & Hochberg, Y. Controlling the False Discovery Rate: A Practical and Powerful Approach to Multiple Testing. *Journal of the Royal Statistical Society Series B: Statistical Methodology***57**, 289–300 (1995).
122. Graham, M. H. CONFRONTING MULTICOLLINEARITY IN ECOLOGICAL MULTIPLE REGRESSION. *Ecology***84**, 2809–2815 (2003).

Figures

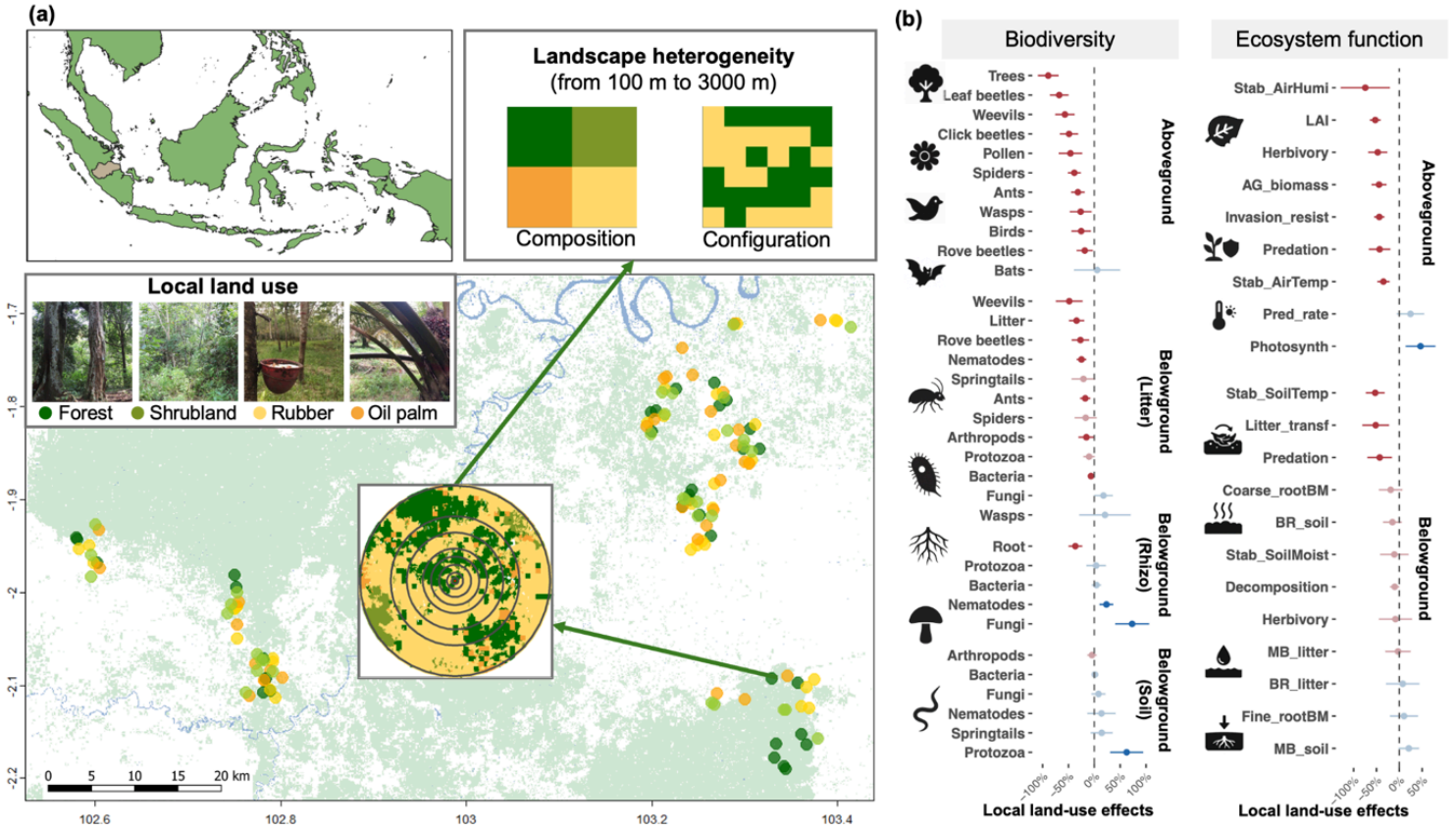


Figure 1

(a) Study design and map of the location of the 128 plots across different land-use systems (rainforest, shrubland, rubber and oil palm plantations) in Sumatra, Indonesia. (b) local land-use effects (plantations vs. rainforest) on the 34 biodiversity indicators and 21 ecosystem functioning indicators across above- and belowground. Bars represent 95% confidence intervals. Colours denote the direction of land-use effects (blue: positive; red: negative), with darker shades indicating statistically significant effects (confidence intervals not overlapping zero) and lighter shades indicating non-significant effects. Abbreviations of ecosystem functioning indicators: *LAI*, leaf area index; *AG_biomass*, aboveground biomass; *Invasion_resist*, resistance to plant invasion; *Pred_rate*, predator attack rate estimated using artificial caterpillars; *Photosynth*, saturated photosynthesis rate; *Litter_transf*, litter transformation rate; *Decomposition*, litter decomposition rate; *Predation* and *Herbivory* denote energy fluxes through predation and herbivory pathways, respectively; *MB*_indicates microbial biomass (*MB_litter*, litter; *MB_soil*, soil); *BR*_indicates basal respiration (*BR_litter*, litter; *BR_soil*, soil); *Fine_rootBM*and *Coarse_rootBM*, fine and coarse root biomass, respectively; *Stab*_indicates (temporal) stability of microclimatic conditions (*Stab_AirHumi*, air humidity; *Stab_AirTemp*, air temperature; *Stab_SoilTemp*, soil temperature; *Stab_SoilMoist*, soil moisture).

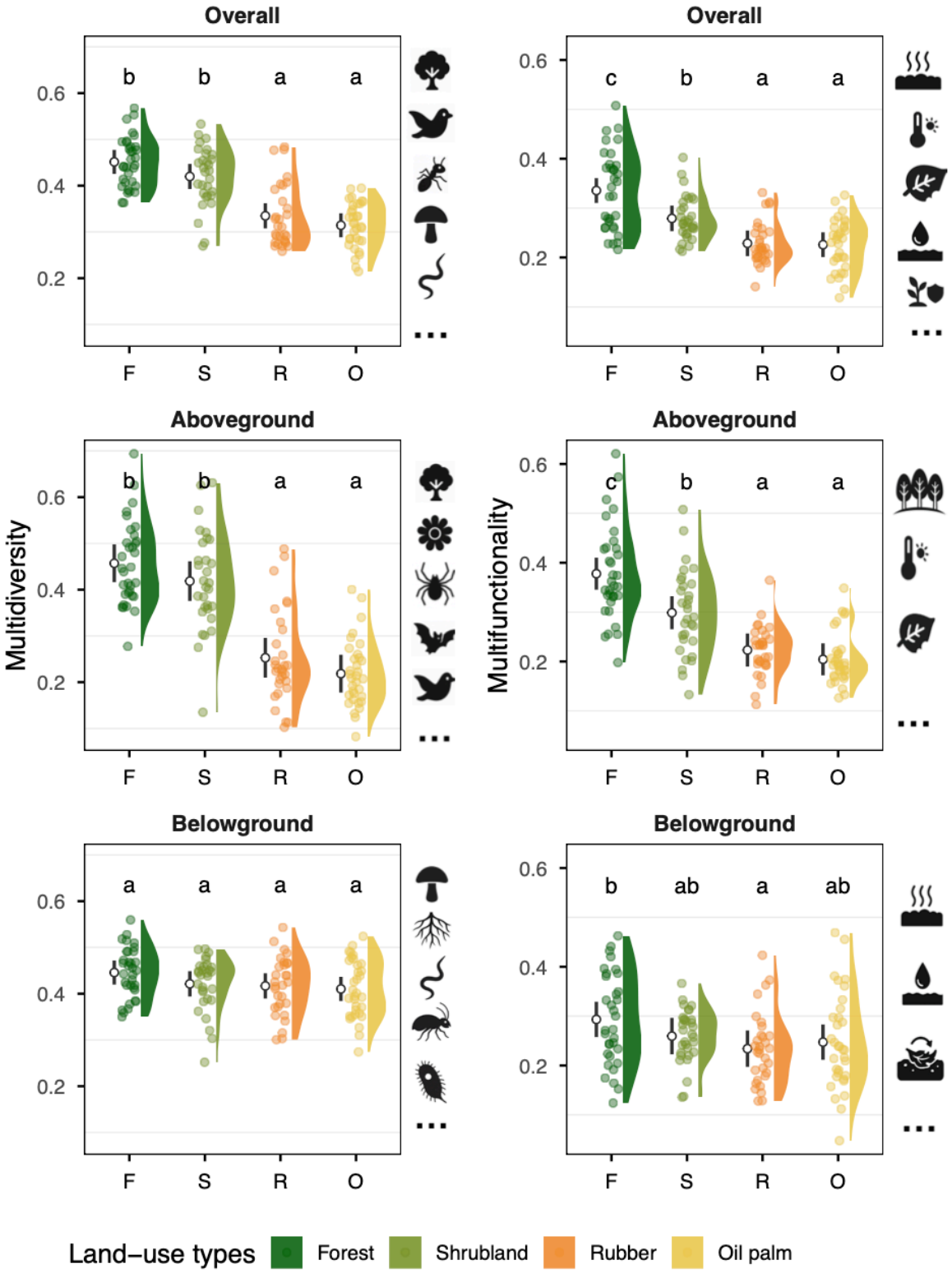


Figure 2

Multidiversity (left panels) and multifunctionality (right panels) across land-use types (forest, shrubland, rubber and oil palm plantations). For both multidiversity and multifunctionality, results are shown for the overall, aboveground and belowground compartments. Overall multidiversity was calculated from 34 indices (including 11 aboveground and 23 belowground indices), whereas overall multifunctionality was calculated from 20 indices (including 8 aboveground and 12 belowground

indices). Colored points represent plot-level values, half-violin plots show the distribution within each land-use type, and open circles with error bars indicate means ± 95% confidence intervals. Different letters indicate significant differences among land-use types within each panel. Results for threshold-based multidiversity and multifunctionality are shown in Fig. S4.

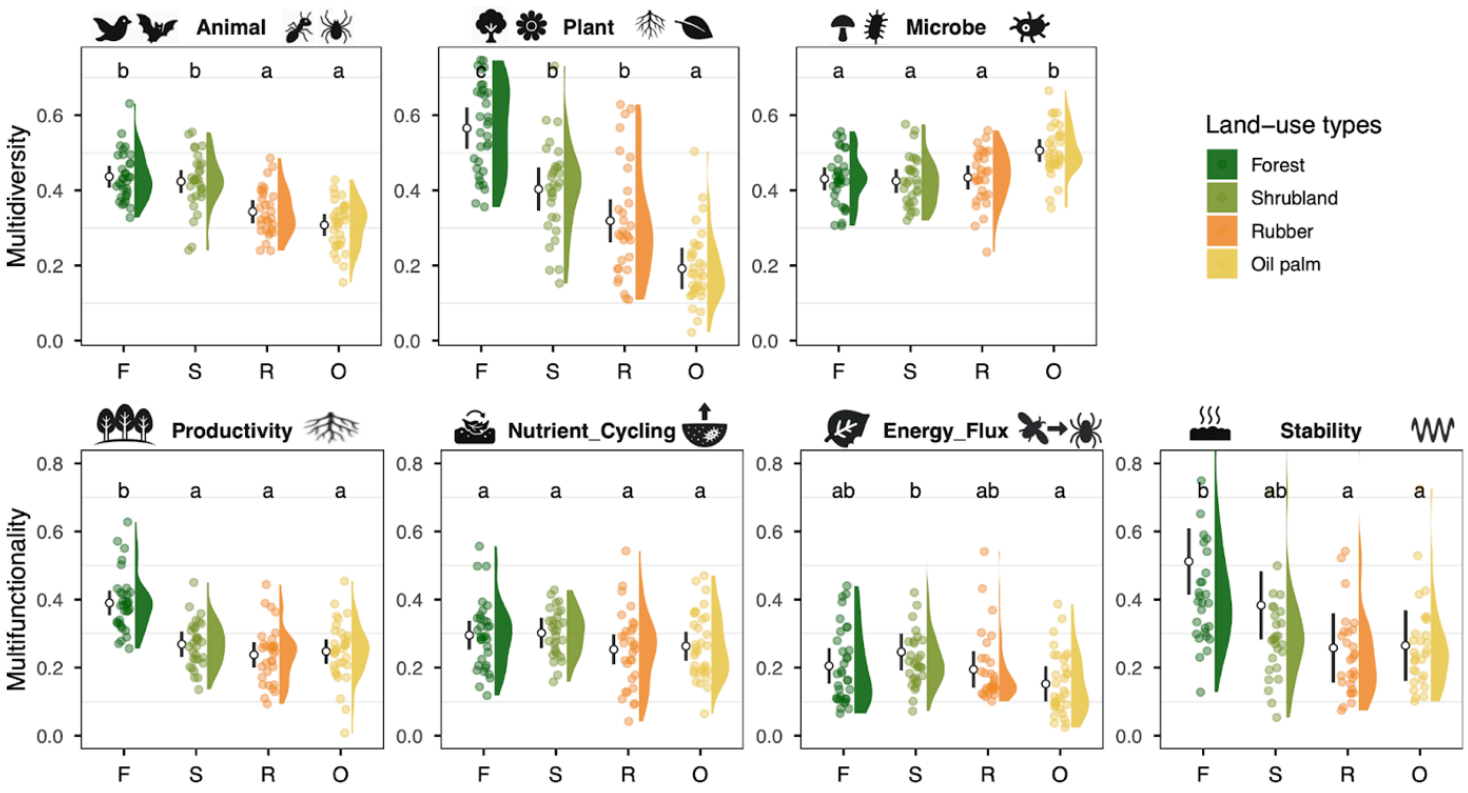


Figure 3

Multidiversity (top panels) and multifunctionality (bottom panels) across land-use types (forest, shrubland, rubber and oil palm plantations). Multidiversity is calculated separately for animals (based on 21 indices), plants (4 indices) and microbial communities (9 indices). Multifunctionality is calculated for productivity (4 indices), nutrient cycling (6 indices), energy flux (5 indices) and resistance (5 indices). Colored points represent plot-level values, half-violin plots show the distribution within each land-use type, and open circles with error bars indicate means ± 95% confidence intervals. Different letters indicate significant differences among land-use types within each panel. Results for threshold-based multidiversity and multifunctionality are presented in Fig. S5.

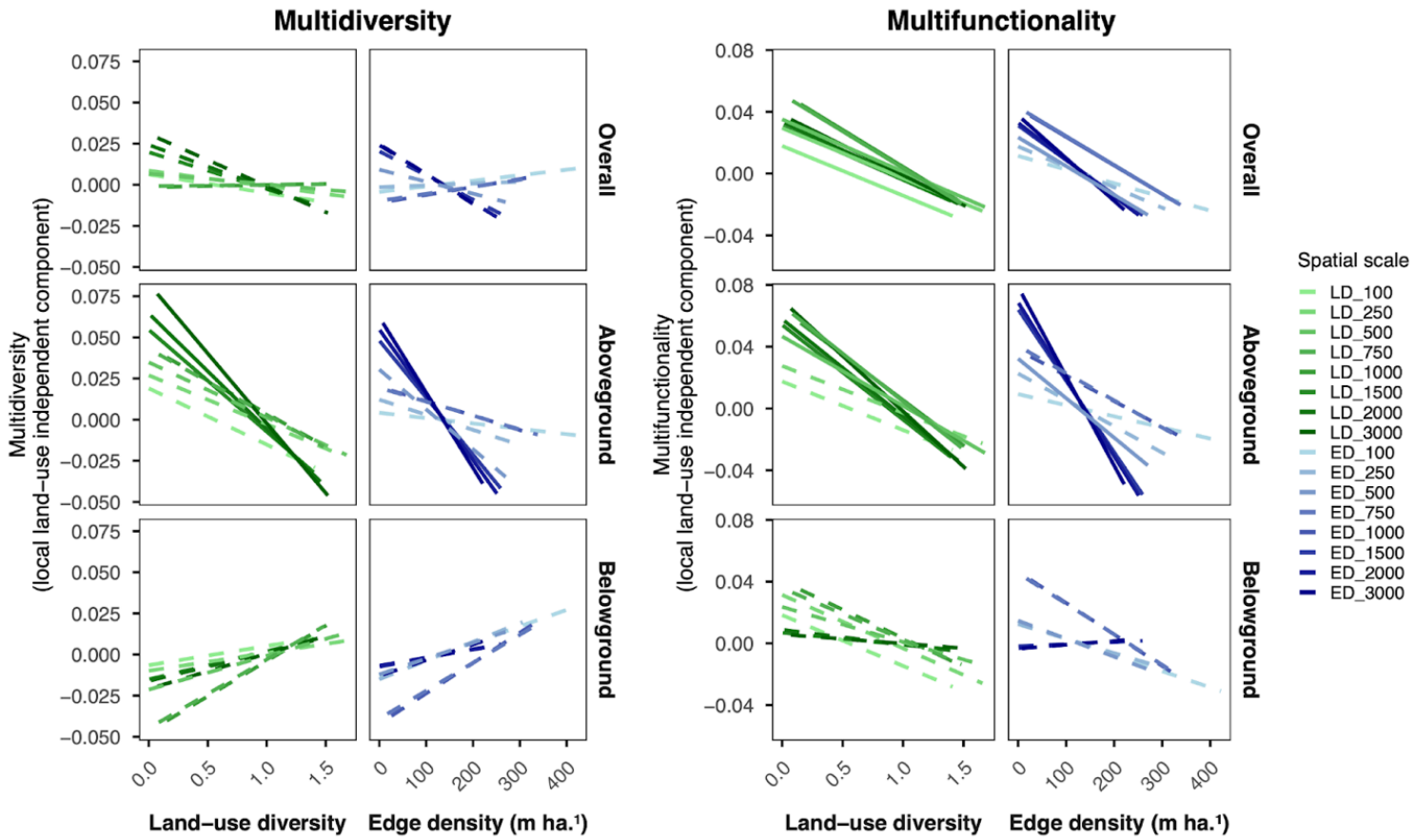


Figure 4

Scale-dependent relationships between landscape heterogeneity and ecosystem multidiversity and multifunctionality. Relationships between the local land-use independent components of multidiversity (left panels) and multifunctionality (right panels) and landscape heterogeneity at multiple spatial scales. Landscape heterogeneity was indicated by both compositional (land-use diversity, LD, green lines) and configurational (edge density, ED, blue) heterogeneity. Solid and dashed lines indicate statistically significant and non-significant relationships, respectively. Significance was assessed using *P*-values adjusted for false discovery rate (FDR) via the Benjamini–Hochberg method.

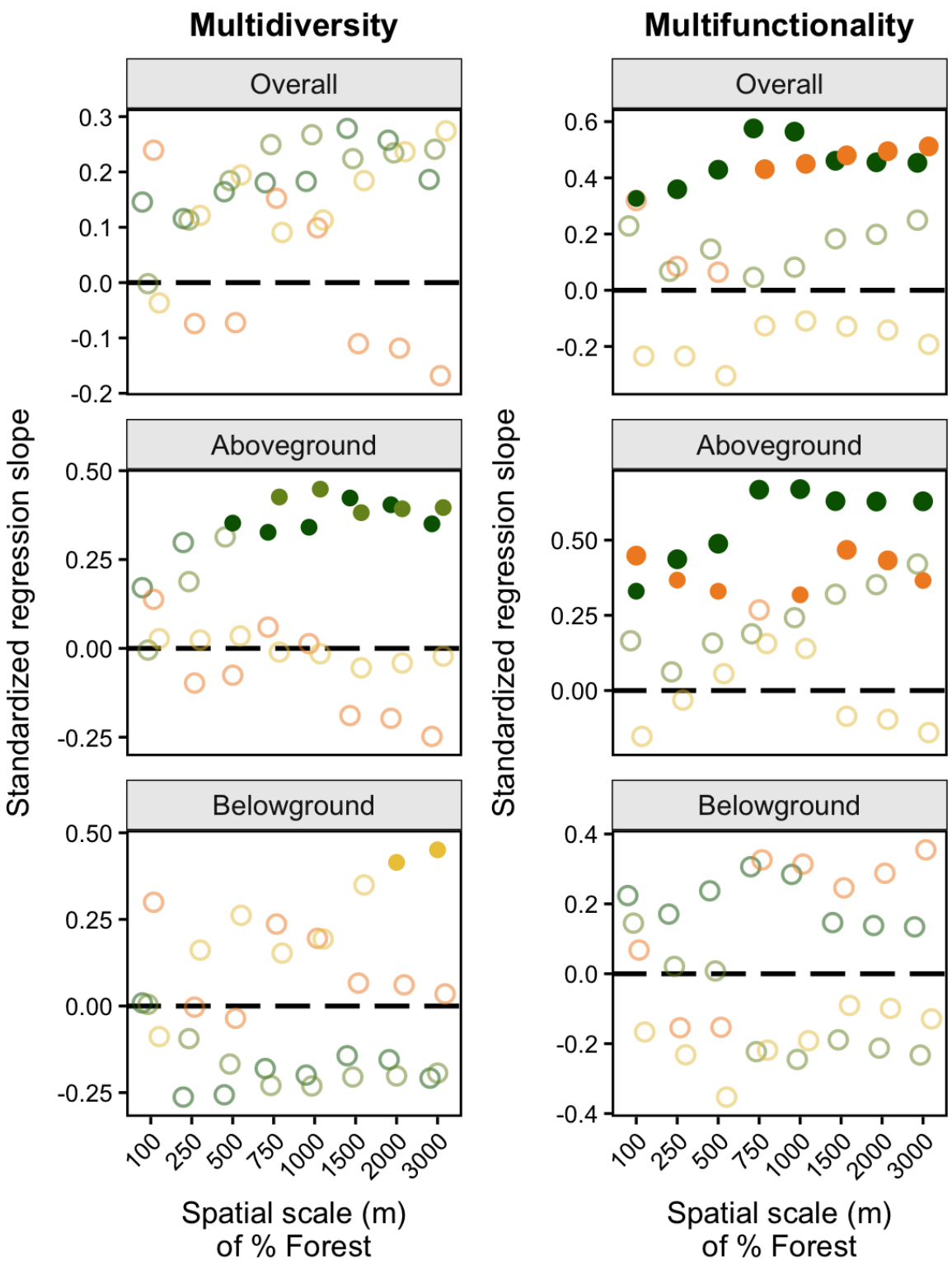


Figure 5

Effect sizes (standardized regression slopes) of rainforest cover on the overall, above- and belowground multidiversity and multifunctionality of plots across local land-use types. The x-axis shows the spatial scale at which rainforest cover was quantified (100–3000 m buffer radius). The y-axis standardized regression slope estimated from a series of linear models fitted separately within each local land-use type. The black dashed line indicates zero effect; points above the line represent positive

relationships, whereas points below the line represent negative relationships. Points are colored according to local land-use type. Significance was assessed using P-values adjusted for false discovery rate (FDR) via the Benjamini–Hochberg method. Filled symbols represent significant results ($P_{adj} < 0.05$), whereas open symbols with reduced transparency represent non-significant ones. Large symbols indicate $P_{adj} < 0.05$ and small symbols indicate $0.05 < P_{adj} < 0.10$.

Supplementary Files

This is a list of supplementary files associated with this preprint. Click to download.

- Supplementaryfiguresandtables.docx